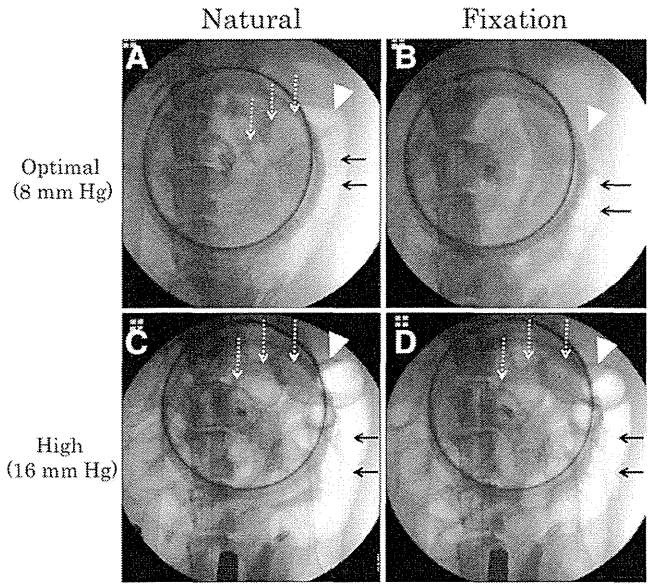


**FIGURE 6.** X-ray images obtained immediately after the insufflation trials for each condition in experiment 2 were completed. Arrowheads indicate each flexure point. Note the distended tracts with migrated gas on the cecal (proximal) side (dotted arrows) and the rectal (distal) side (solid arrows). A, In the natural model with optimal insufflation pressure, gas migration was observed in the oral tract around the cecum. B, In the fixation model with optimal insufflation pressure, gas migration was confirmed only at the rectal side of the colon; gas was not observed at the oral side beyond the flexure point. C, In the natural model with high insufflation pressure, gas migration was observed in the oral tract around the cecum and the distal ileum. D, In the fixation model with high insufflation pressure, gas migration was confirmed at the oral side beyond the flexure point around the cecum.

SPACE exhibited no major migration of gas to the small bowel. In contrast, conventional manual insufflation colonoscopy resulted in significant gas migration to the small bowel (Fig. 4). This was partially documented by the significant changes in pH and arterial partial pressure of carbon dioxide after 20 minutes of manual versus automatic insufflation (Table 1). This difference in gas migration was considered compatible with our previous report on upper GI SPACE[4] and is considered an important feature of SPACE.

The results of experiment 2 supplement our understanding of the underlying mechanism that enables SPACE colonoscopy without massive gas migration. We found that anatomic flexure and optimal insufflation pressure were important factors to prevent gas migration; rectal SPACE was only successful (without gas migration to the upper colonic segments) in the presence of anatomic flexure and adequate insufflation pressure. Under adequate insufflation pressure, the flexure may act as a pressure valve that temporarily prevents gas migration. This hypothesis was supported by our radiologic results; the confinement of insufflated gas was only observed in fixation models with optimal pressure insufflation (Fig. 6). However, the valvular mechanism mentioned above might not effectively prevent gas migration, when the insufflation pressure overcomes its anatomic barrier. Our data suggest that such a pressure threshold for successful rectal SPACE may exist between 8 and 16 mm Hg in canines. In human subjects, it has been clinically proven that the use of 20 to 30 mm Hg of rectal insufflation pressure causes diffuse gas extension throughout the entire colon, which enables computed tomographic colonography.[22] Additional evaluations are required to establish the optimal insufflation pressure for each segment of the lower GI tract.

SPACE colonoscopy may be feasible in the human lower GI tract, in which the valvular mechanism would work under optimal insufflation pressure depending on flexures such as the sigmoid-descending colon junction, splenic flexure, and hepatic flexure. The small amount of gas migration to the upstream bowel may reduce abdominal bloating and discomfort. Even during complications such as intestinal perforation during colonoscopy, excessive insufflation into the peritoneal cavity (which might lead to abdominal compartment syndrome) could be avoided by metered and computer-mediated insufflation. We believe that SPACE will become a key insufflation modality in the lower GI tract, especially in complicated endoscopic treatments like ESD.

Although we confirmed interesting findings in SPACE colonoscopy, this study had some limitations. This was an animal study with a relatively small sample size. No feedback was available regarding distention because all of the procedures were performed under general anesthesia. In actual clinical practice, optimal insufflation pressure should be confirmed in each segment of the lower GI tract, incorporating clinical feedback from patients regarding pain, distention, and discomfort. Because the maximum duration of insufflation was 20 minutes, additional studies are required to confirm the effects of longer-duration SPACE colonoscopy, especially on cardiopulmonary parameters. Moreover, some ancillary devices may be required in human settings. Because the UHI-3 was originally designed for intra-abdominal use, a dedicated insufflation device for the GI tract should be developed. Any antileak device, such as the rectal overtube used in our study, would also be necessary in the clinical setting. We used a crude, handmade rectal tube and had slight difficulty inserting and withdrawing the scope. These issues should be addressed before the clinical introduction of SPACE colonoscopy. After confirmation of the feasibility and safety of SPACE colonoscopy in human subjects, a multicenter, randomized clinical trial comparing the outcome of colonic ESD under manual $CO_2$ insufflation versus SPACE would be required to confirm the genuine benefits of SPACE colonoscopy.

## CONCLUSION

This study confirmed that SPACE colonoscopy is feasible and safe in canine models. SPACE provided stable and highly reproducible endoscopic exposure and working space. Gas was confined to the insufflated segment of the GI tract in the presence of intestinal flexure and optimal insufflation pressure, suggesting that contributing factors are anatomic barrier and pressure setting. Additional assessments are needed to optimize SPACE and to apply this potentially attractive new modality to humans.

## ACKNOWLEDGEMENTS

The authors are grateful to Nobuyuki Torisawa (Fujifilm, Tokyo, Japan) for his technical assistance.

## REFERENCES

1. Uraoka T, Parra-Blanco A, Yahagi N. Colorectal endoscopic submucosal dissection: is it suitable in Western countries? *J Gastroenterol Hepatol.* 2013;28:406–414.
2. Swanstrom LL. NOTES: Platform development for a paradigm shift in flexible endoscopy. *Gastroenterology.* 2011;140:1150–1154.e1.
3. Nakajima K, Nishida T, Milsom JW, et al. Current limitations in endoscopic $CO_2$ insufflation for NOTES: flow and pressure study. *Gastrointest Endosc.* 2010;72:1036–1042.
4. Nakajima K, Moon JH, Tsutsui S, et al. Esophageal submucosal dissection under steady pressure automatically controlled endoscopy (SPACE): a randomized preclinical trial. *Endoscopy.* 2012;44:1139–1148.
5. Uraoka T, Kawahara Y, Kato J, Saito Y, Yamamoto K. Endoscopic submucosal dissection in the colorectum: present status and future prospects. *Dig Endosc.* 2009;21(suppl 1):S13–S16.
6. Yoshida N, Yagi N, Naito Y, Yoshikawa T. Safe procedure in endoscopic submucosal dissection for colorectal tumors focused on preventing complications. *World J Gastroenterol.* 2010;16:1688–1695.
7. Scheppach W. The abdominal compartment syndrome - widely unknown in gastroenterology [in German]. *Z Gastroenterol.* 2007;45:321–324.
8. Souadka A, Mohsine R, Ifrine L, Belkouchi A, El Malki HO. Acute abdominal compartment syndrome complicating a colonoscopic perforation: a case report. *J Med Case Rep.* 2012;6:51.
9. Stevenson GW, Wilson JA, Wilkinson J, Norman G, Goodacre RL. Pain following colonoscopy: elimination with carbon dioxide. *Gastrointest Endosc.* 1992;38:564–567.
10. Williams CB. Who's for CO2? *Gastrointest Endosc.* 1986;32:365–367.
11. Dellon ES, Hawk JS, Grimm IS, Shaheen NJ. The use of carbon dioxide for insufflation during GI endoscopy: a systematic review. *Gastrointest Endosc.* 2009;69:843–849.
12. Hilzenrat N, Fich A, Odes HS, et al. Does insertion of a rectal tube after colonoscopy reduce patient discomfort and improve satisfaction? *Gastrointest Endosc.* 2003;57:54–57.
13. Rogers BH. The safety of carbon dioxide insufflation during colonoscopic electrosurgical polypectomy. *Gastrointest Endosc.* 1974;20:115–117.
14. Bretthauer M, Thiis-Evensen E, Huppertz-Hauss G, et al. NORCCAP (Norwegian colorectal cancer prevention): a randomised trial to assess the safety and efficacy of carbon dioxide versus air insufflation in colonoscopy. *Gut.* 2002;50:604–607.
15. Bretthauer M, Lynge AB, Thiis-Evensen E, Hoff G, Fausa O, Aabakken L. Carbon dioxide insufflation in colonoscopy: safe and effective in sedated patients. *Endoscopy.* 2005;37:706–709.
16. Saito Y, Uraoka T, Matsuda T, et al. A pilot study to assess the safety and efficacy of carbon dioxide insufflation during colorectal endoscopic submucosal dissection with the patient under conscious sedation. *Gastrointest Endosc.* 2007;65:537–542.
17. Omori T, Nakajima K, Ohashi S, et al. Laparoscopic intragastric surgery under carbon dioxide pneumostomach. *J Laparoendosc Adv Surg Tech A.* 2008;18:47–51.
18. Yasumasa K, Nakajima K, Endo S, Ito T, Matsuda H, Nishida T. Carbon dioxide insufflation attenuates parietal blood flow obstruction in distended colon: potential advantages of carbon dioxide insufflated colonoscopy. *Surg Endosc.* 2006;20:587–594.
19. Nakajima K, Yasumasa K, Endo S, et al. A versatile dual-channel carbon dioxide (CO2) insufflator for various CO2)applications: the prototype. *Surg Endosc.* 2006;20:334–338.
20. Souma Y, Nakajima K, Takahashi T, et al. The role of intraoperative carbon dioxide insufflating upper gastrointestinal endoscopy during laparoscopic surgery. *Surg Endosc.* 2009;23:2279–2285.
21. Bretthauer M, Seip B, Aasen S, Kordal M, Hoff G, Aabakken L. Carbon dioxide insufflation for more comfortable endoscopic retrograde cholangiopancreatography: a randomized, controlled, double-blind trial. *Endoscopy.* 2007;39:58–64.
22. Sosna J, Bar-Ziv J, Libson E, Eligulashvili M, Blachar A. CT colonography: positioning order and intracolonic pressure. *AJR Am J Roentgenol.* 2008;191:1100.

# Expression of insulin-like growth factor-II mRNA-binding protein-3 as a marker for predicting clinical outcome in patients with esophageal squamous cell carcinoma

AKIHIRO TAKATA[1], SHUJI TAKIGUCHI[1], KAORU OKADA[2], TSUYOSHI TAKAHASHI[1], YUKINORI KUROKAWA[1], MAKOTO YAMASAKI[1], HIROSHI MIYATA[1], KIYOKAZU NAKAJIMA[1], MASAKI MORI[1] and YUICHIRO DOKI[1]

[1]Department of Gastroenterological Surgery, Graduate School of Medicine, Osaka University, Suita, Osaka 565-0871; [2]Department of Surgery, Nishinomiya Municipal Central Hospital, Nishinomiya, Hyogo 663-8014, Japan

Received November 12, 2013; Accepted June 19, 2014

DOI: 10.3892/ol.2014.2465

**Abstract.** Insulin-like growth factor-II mRNA-binding protein-3 (IMP3) is an important factor in carcinogenesis, although its clinical significance in esophageal squamous cell carcinoma (ESCC) remains unknown. The present study investigated the associations between IMP3 expression and the clinicopathological parameters. IMP3 expression was assessed in 191 resected ESCC specimens, and the associations between IMP3 expression in ESCC, the clinicopathological parameters and patient prognosis were examined. Using immunohistochemistry, 113 (59.2%) tumors were identified as IMP3-positive. IMP3 positivity correlated significantly with high pathological (p)Stage, pT stage and pN stage. The IMP3-positive patients exhibited a poorer prognosis compared with the IMP3-negative patients. In univariate analyses, histology [hazard ratio (HR), 1.94; 95% confidence interval (CI), 1.18-3.49; P=0.0082], pT (HR, 2.34; 95% CI, 1.55-3.62; P<0.0001), pN (HR, 2.85; 95% CI, 1.81-4.69; P<0.0001), lymphatic invasion (HR, 2.08; 95% CI, 1.26-3.70; P=0.0036), venous invasion (HR, 1.79; 95% CI, 1.21-2.64; P=0.0039), neoadjuvant chemotherapy (NAC) (HR, 2.01; 95% CI, 1.35-3.00; P=0.0005) and IMP3 expression (HR, 2.12; 95% CI, 1.40-3.29; P=0.0003) were significantly associated with overall survival. Using multivariate analyses, histology (HR, 1.87; 95% CI, 1.13-3.29; P=0.014), pN (HR, 2.19; 95% CI, 1.36-3.66; P=0.0010), NAC (HR, 1.88; 95% CI, 1.24-2.86; P=0.0028) and IMP3 expression (HR, 1.84; 95% CI, 1.18-2.93; P=0.0064) were significant prognostic factors. IMP3 may therefore be a prognostic factor for patients with ESCC who have undergone a curative resection.

*Correspondence to:* Dr Shuji Takiguchi, Department of Gastroenterological Surgery, Graduate School of Medicine, Osaka University, 2-2, E2, Yamadaoka, Suita, Osaka 565-0871, Japan
E-mail: stakiguchi@gesurg.med.osaka-u.ac.jp

*Key words:* insulin-like growth factor-II mRNA-binding protein-3, esophageal squamous cell carcinoma, immunohistochemistry

## Introduction

In East Asian countries, esophageal squamous cell carcinoma (ESCC) is the major histological form of esophageal cancer. The disease is also one of the most lethal digestive tract malignances (1). In the majority of cases, the initial diagnosis of ESCC is made when the malignancy has already progressed to an advanced stage (1). Despite recent improvements in multi-treatment approaches, including surgery, radiotherapy and chemotherapy, the prognosis for patients with ESCC remains unsatisfactory (2). Predicting a prognosis by examining the clinicopathological characteristics remains difficult, even when using the tumor-node-metastasis staging system. This is due to considerable tumor variability and heterogeneity within the same pathological stage.

The IMP3 gene, also known as the K homology domain-containing gene (KOC) or L523S, encodes the IMP3 protein (3). IMP3 is located on chromosome 7p11.5 and encodes a 4350-bp mRNA and a 580-aa protein. IMP3 is expressed in the developing epithelium, muscle and placenta during the early stages of human and mouse embryogenesis, and low or undetectable levels of IMP3 are present in adult tissues (4,5). IMP3 has been shown to be overexpressed in testicular cancer, renal cell carcinoma, ovarian carcinoma, gastric cancer, colon cancer and adenocarcinoma of the lung (6-15). The IMP3 protein, together with IMP-1 and IMP-2, has different functions in various post-transcriptional processes, including mRNA localization, mRNA turnover and translational control (16-19). The IMP3 gene has previously been used as a marker to detect malignant cells in fine-needle aspirates (20). Additionally, in K562 leukemia cells, the inhibition of IMP3 has been shown to result in apoptosis, indicating that it may be vital for cancer cell survival (18). IMP3 is a prognostic biomarker in patients with endometrial serous carcinoma and renal cell carcinoma. In such cases, IMP3 expression appears to predict an increased likelihood of metastasis following surgery and a shorter metastasis-free survival time (8-11,15). However, to the best of our knowledge, the clinicopathological and prognostic significance of IMP3 expression in ESCC remains unknown. In the present study, the prevalence and clinicopathological significance of IMP3 expression were investigated with regard

to overall survival (OS) and recurrence-free survival (RFS) in 191 patients.

## Materials and methods

*Patients and treatments.* The present study examined 191 patients with pathologically confirmed primary ESCC who underwent surgical resection at the Osaka University Hospital (Osaka, Japan) between 1998 and 2007 (Table I). Approval for the study was obtained from the Ethics Committee of Osaka University Hospital. The study population consisted of 24 female and 167 male patients who ranged between 29 and 85 years of age (median, 62.7 years). All patients underwent a subtotal esophagectomy via a right thoracotomy, with a two- or three-field lymphadenectomy, with curative resection. None of the patients succumbed to post-operative complications. Of the 104 patients with lymph node metastases at the initial diagnosis, 86 received neoadjuvant chemotherapy (NAC), which consisted of two courses of 5-fluorouracil (700 mg/m$^2$ on days one to seven), cisplatin (70 mg/m$^2$ on day one) and Adriamycin (35 mg/m$^2$ on day one). Following surgery, the patients were followed up every 3 months by physical examination and an analysis of serum tumor markers (squamous cell carcinoma antigen and carcinoembryonic antigen), every 6 months by computed tomography scanning and abdominal ultrasonography, and every year by endoscopy until tumor recurrence became evident. Patients exhibiting tumor recurrence received chemotherapy or chemoradiotherapy for as long as this regimen was systemically tolerated. The mean OS time was 41 months, and the mean RFS time was 39 months.

*Immunohistochemical analysis.* IMP3 expression was examined in formalin-fixed, paraffin-embedded ESCC tissue sections by immunohistochemistry (IHC). One representative slide with the deepest tumor invasion was selected from each patient and examined by IHC. The tissue sections were deparaffinized in xylene and then rehydrated through a graded ethanol series. For antigen retrieval, the slides were incubated by autoclaving at 110˚C in 10 mm Tris and 1 mm EDTA buffer (pH 9.0) for 20 min. Endogenous peroxidase activity was blocked with 0.3% $H_2O_2$ in methanol for 20 min and non-specific binding was blocked with 10% normal serum for 20 min. Subsequently, the tissue slides were incubated overnight with anti-IMP3 antibody (monoclonal mouse anti-human L523S; dilution, 1:200; Dako Cytomation, Carpinteria, CA, USA) at 4˚C in a humidified chamber. The bound antibody was visualized using the Avidin/Biotin Complex Peroxidase Detection System (Vector Laboratories, Burlingame, CA, USA). Finally, the sections were incubated in 3,3'-diaminobenzidine tetrahydrochloride with 0.05% $H_2O_2$ for 3 min and counterstained with 0.1% hematoxylin. IMP3 staining for each ESCC sample was defined as positive when >10% of the cancer cells in the section were immunoreactive with the anti-IMP3 antibody. Staining was defined as negative when ≤10% of the cancer cells in the section were positive.

*Statistical analysis.* Statistical analysis was performed using JMP software (JMP version 9.0.2; SAS Institute, Cary, NC, USA). The association between IMP3 expression and the clinicopathological parameters was assessed using the $\chi^2$ test. The RFS and OS were assessed using the Kaplan-Meier method and compared using the log-rank test. All the parameters that were found to be significant in a univariate analysis using the Cox proportional hazard model were entered into a multivariate survival analysis. P-values were derived from two-tailed testing and $P<0.05$ was considered to indicate a statistically significant difference.

Table I. Characteristics of patients with ESCC.

| Parameters | Value |
|---|---|
| Median age, years (range) | 62.7 (29-85) |
| Gender, n (%) | |
| Male | 167 (87.4) |
| Female | 24 (12.6) |
| Histology of SCC, n (%) | |
| Poorly-differentiated | 45 (23.6) |
| Moderately-differentiated | 99 (51.8) |
| Well-differentiated | 47 (24.6) |
| Pathological classification[a], n (%) | |
| pT | |
| 0 | 0 (0.0) |
| 1 | 51 (26.7) |
| 2 | 30 (15.7) |
| 3 | 93 (48.7) |
| 4 | 17 (8.9) |
| pN | |
| N0 | 68 (35.6) |
| N1 | 53 (27.7) |
| N2 | 35 (18.3) |
| N3 | 35 (18.3) |
| pStage | |
| 0 | 0 (0.0) |
| I | 39 (20.4) |
| II | 53 (27.7) |
| III | 63 (33.0) |
| IV | 36 (18.8) |

[a]According to the Union for International Cancer Control, 7th edition (21). ESCC; esophageal squamous cell carcinoma; pN; pathological N stage; pT, pathological T stage; pStage, pathological stage.

## Results

*IMP3 expression in ESCC.* A total of 191 samples that contained cancerous and non-cancerous lesions were evaluated for IMP3 expression using IHC. Of these, 113 (59.2%) showed positive IMP3 expression that was predominantly localized to the cytoplasm of the tumor cells, along with faint nuclear staining (Fig. 1A). The remaining 78 (40.8%) were negative for

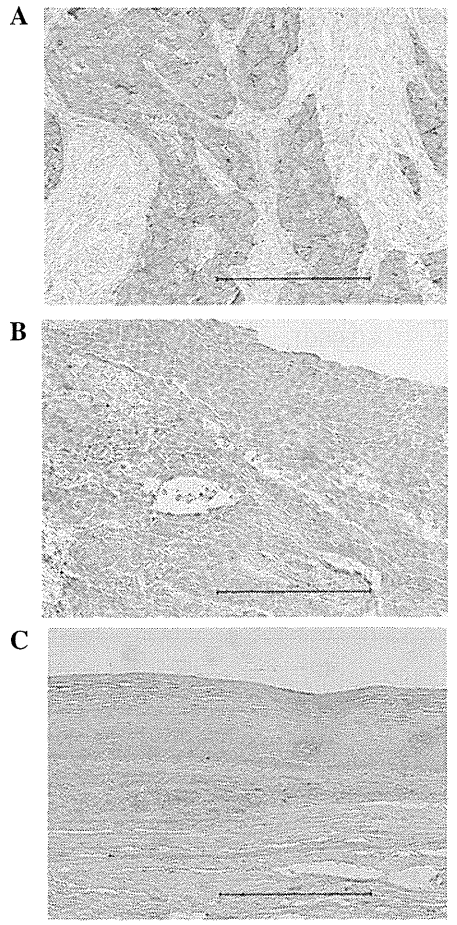


Figure 1. Representative images of IMP-3 expression, as determined by immunohistochemical staining. (A) IMP-3-positive esophageal squamous cell carcinoma exhibiting staining mainly in the cytoplasm of the tumor cells. (B) IMP-3-negative esophageal squamous cell carcinoma exhibiting almost no staining of the tumor cells. (C) Normal squamous epithelium negative for IMP-3. The black scale bar represents 250 $\mu$M. IMP3, insulin-like growth factor-II mRNA-binding protein-3.

IMP3 expression (Fig. 1B). The positive staining was almost homogeneous in individual cancer foci and in different areas, such as in the surface, central and deepest areas, of the cancer lesions. By contrast, none of the normal squamous epithelia exhibited substantial IMP3 staining, although certain basal cells showed faint nuclear staining (Fig. 1C).

*Association between IMP3 expression and clinicopathological parameters.* Table II lists the associations between IMP3 expression and the clinicopathological parameters. The IMP3-positive tumors were significantly associated with deeper tumor invasion and lymph node metastases compared with the IMP3-negative tumors (P=0.0001 and P=0.026, respectively). No significant associations were observed between IMP3 expression and other parameters, including age, gender, histology and use of NAC.

*Association between IMP3 expression and survival.* The 5-year OS rate of the population was 48.5%. Patients with IMP3-positive tumors experienced a poorer 5-year OS rate compared with those with IMP3-negative tumors (39.3 vs. 61.7%, P=0.0004; Fig. 2A). Similarly, patients with IMP3-positive tumors experienced a poorer RFS rate compared with those with IMP3-negative tumors (35.7 vs. 61.9%, P=0.0004; Fig. 2B). By univariate analyses, histology [hazard ratio (HR), 1.94; 95% confidence interval (CI), 1.18-3.49; P=0.0082], pathological T stage (pT; HR, 2.34; 95% CI, 1.55-3.62; P<0.0001), pathological N stage (pN; HR, 2.85; 95% CI, 1.81-4.69; P<0.0001), lymphatic invasion (HR, 2.08; 95% CI, 1.26-3.70; P=0.0036), venous invasion (HR, 1.79; 95% CI, 1.21-2.64; P=0.0039), NAC (HR, 2.01; 95% CI, 1.35-3.00; P=0.0005), and IMP expression (HR, 2.12; 95% CI, 1.40-3.29; P=0.0003) were significantly correlated with OS (Table III). The seven parameters that demonstrated statistical significance (P<0.05) by univariate analysis were further analyzed by multivariate analysis. Multivariate analysis showed that pathological lymph node metastasis was the poorest prognostic factor (HR, 2.19; 95% CI, 1.36-3.66; P=0.0010), followed by NAC (HR, 1.88;

Table II. Correlation between IMP3 expression and clinicopathological parameters.

| | IMP3 expression, n (%) | | |
|---|---|---|---|
| Parameters | Positive | Negative | P-value |
| Age, years | | | |
| <65 | 64 (33.5) | 47 (24.6) | 0.6179 |
| ≥65 | 49 (25.7) | 31 (16.2) | |
| Gender | | | |
| Male | 97 (50.8) | 70 (36.6) | 0.4191 |
| Female | 16 (8.4) | 8 (4.2) | |
| Histology[a] | | | |
| Poor/moderate | 89 (46.6) | 55 (28.8) | 0.1955 |
| Well | 24 (12.6) | 23 (12.0) | |
| Neoadjuvant chemotherapy | | | |
| Yes | 48 (25.1) | 38 (19.9) | 0.4654 |
| No | 65 (34.0) | 40 (20.9) | |
| Depth of tumor invasion[b] | | | |
| pT1-2 | 35 (18.3) | 46 (24.1) | 0.0010 |
| pT3-4 | 78 (40.8) | 32 (16.8) | |
| Lymph node metastasis[b] | | | |
| pN0 | 33 (17.3) | 35 (18.3) | 0.0267 |
| pN1-3 | 80 (41.9) | 43 (22.5) | |
| pStage[b] | | | |
| I, II | 67 (35.1) | 46 (24.1) | 0.0003 |
| III, IV | 46 (24.1) | 32 (16.8) | |

[a]Well-, moderately- and poorly-differentiated squamous cell carcinoma. [b]According to the Union for International Cancer Control, 7th edition (21). pN; pathological N stage; pT, pathological T stage; pStage, pathological stage; IMP3, insulin-like growth factor-II mRNA-binding protein-3.

Table III. Univariate and multivariate analysis of OS using Cox's proportional hazard model.

| Parameter | Number of cases | Univariate | | Multivariate | |
|---|---|---|---|---|---|
| | | HR (95% CI) | P-value | HR (95% CI) | P-value |
| Age (>65 years) | 78/113 | 1.24 (0.84-1.84) | 0.2766 | | |
| Gender (female/male) | 24/167 | 1.05 (0.56-1.82) | 0.8591 | | |
| Histology (poor-moderate/well)[a] | 144/47 | 1.94 (1.18-3.49) | 0.0082 | 1.87 (1.13-3.29) | 0.0134 |
| pT (T3,4/T1,2)[b] | 110/81 | 2.34 (1.55-3.62) | <0.0001 | 1.28 (0.79-2.10) | 0.3303 |
| pN (N1-3, N0)[b] | 123/68 | 2.85 (1.81-4.69) | <0.0001 | 2.19 (1.36-3.66) | 0.0010 |
| Lympathic invasion (present/absent) | 148/43 | 2.08 (1.26-3.70) | 0.0036 | 1.11 (0.62-2.08) | 0.7354 |
| Venous invasion (present/absent) | 79/112 | 1.79 (1.21-2.64) | 0.0039 | 1.22 (0.79-1.91) | 0.3740 |
| NAC (yes/no) | 86/105 | 2.01 (1.35-3.00) | 0.0005 | 1.88 (1.24-2.86) | 0.0028 |
| IMP3 expression (positive/negative) | 113/78 | 2.12 (1.40-3.29) | 0.0003 | 1.84 (1.18-2.93) | 0.0064 |

[a]Well-, moderately- and poorly-differentiated squamous cell carcinoma. [b]According to the Union for International Cancer Control, 7th edition (21). OS, overall survival; pN; pathological N stage; pT, pathological T stage; HR, hazard ratio; CI, confidence interval; IMP3, insulin-like growth factor-II mRNA-binding protein-3; NAC, neoadjuvant chemotherapy.

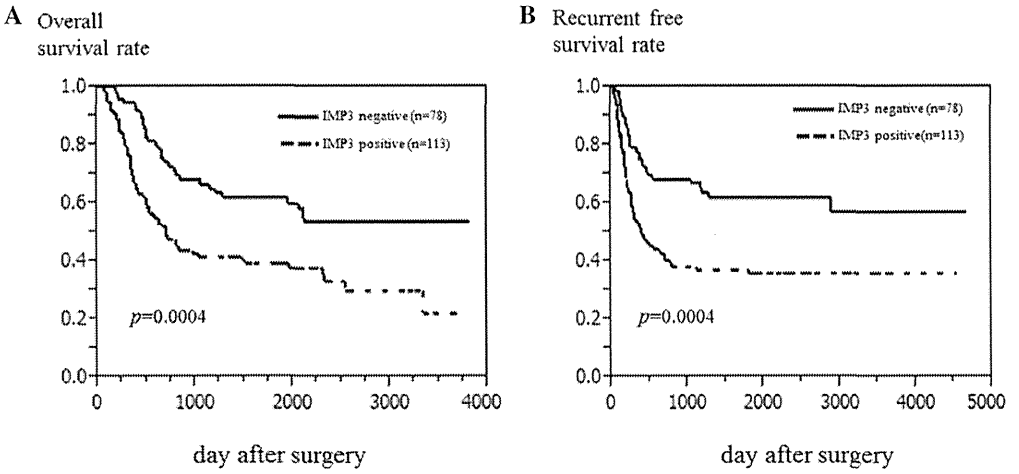


Figure 2. Survival curves according to IMP-3 expression. (A) Overall survival of all patients was plotted using the Kaplan-Meier method. (B) Recurrence-free survival of all patients. IMP3, insulin-like growth factor-II mRNA-binding protein-3.

95% CI, 1.24-2.86; P=0.0028), histology (HR, 1.87; 95% CI, 1.13-3.49; P=0.014), and IMP3 expression (HR, 1.84; 95% CI, 1.18-2.93; P=0.0064) (Table III).

## Discussion

IMP3 is an RNA-binding protein and a KH domain-containing member of the IMP family. In mice, IMPs are primarily expressed during early embryogenesis and at mid-gestation, but they are not expressed in the majority of adult human tissues (3,4,22). IMP3 has been reported to function by regulating tumor cell proliferation, migration and metastasis. IMP3 has been shown to promote tumor cell proliferation through the upregulation of IGF2, a potent mitogenic factor previously shown to exert effects in a number of diseases (18,23,24). Studies have additionally found that IMP3 can exert a marked effect on cellular adhesion and invasion during normal development and during the development of cancers (25). For these reasons, strong IMP3 expression is regarded as an indicator of a poor prognosis (6,9,10,26,27). However, to the best of our knowledge, the clinicopathological and prognostic significance of IMP3 expression in ESCC has not been reported.

The present study demonstrated the positive immunoreactivity to IMP3 of 59.2% of ESCC surgical samples. Positive IMP3 expression was significantly associated with pathological factors associated with tumor progression [pT, pN and pathological stage (pStage)]. IMP3 was identified as a prognostic factor for OS. Although pT is generally considered to be an independent prognostic factor, this was not the case in the present series. In the present study, patients with advanced ESCC received NAC. Hence, the effect of pT was canceled by the effect of NAC in the multivariate analysis. This result was similar to that reported in other cancers (6,9-11,26,27). However, the clinical association between IMP3 and a worse prognosis of ESCC remains poorly defined. Yoshino *et al* (28) reported that IMP3 mRNA expression was associated with

resistance to radiation therapy in ESCC cell lines. Further studies to investigate this should therefore be performed in the future.

Several characteristics of IMP3 indicate that it may be a potentially attractive prognostic marker. First, IMP3 IHC staining is a simple and reliable assay to perform (9). In the majority of cases, carcinomas are treated surgically, allowing chemotherapy and radiation therapy to be combined. Tumor tissues are thus routinely available for IHC staining using the monoclonal L523 antibody. The present study found that IMP3 IHC was reproducible and could be readily performed on ESCC tissues. The simplicity of this assay will enable a pre-operative diagnosis from the analysis of biopsy tissue. Regarding the polymerase chain reaction (PCR)-based method, IMP3 has been used as a molecular marker to predict peritoneal recurrence following curative surgery for gastric cancer (11), and PCR amplification of IMP3 from biliary structure specimens have been useful to distinguish between benign and malignant lesions (29). Furthermore, IMP3 has been considered a potential target for immunotherapy. A phase II study using a peptide vaccine therapy, which included IMP3, has been performed for patients with advance ESCC who failed to respond to standard therapies (30). It has been reported that the immune response induced by the vaccination may improve the prognosis for patients with advanced ESCC.

In conclusion, in the present study, IMP3, a novel mRNA-binding protein, was shown to be frequently expressed in ESCC. IMP3 expression was more commonly observed in ESCC patients with poor prognostic factors. IMP3 may be a potential IHC biomarker that can be used to evaluate the tumor progression and prognosis of ESCC.

## References


1. Shimada H, Nabeya Y, Okazumi S, *et al*: Prediction of survival with squamous cell carcinoma antigen in patients with resectable esophageal squamous cell carcinoma. Surgery 133: 486-494, 2003.
2. Tamoto E, Tada M, Murakawa K, *et al*: Gene-expression profile changes correlated with tumor progression and lymph node metastasis in esophageal cancer. Clin Cancer Res 10: 3629-3638, 2004.
3. Nielsen J, Christiansen J, Lykke-Andersen J, *et al*: A family of insulin-like growth factor II mRNA-binding proteins represses translation in late development. Mol Cell Biol 19: 1262-1270, 1999.
4. Mueller-Pillasch F, Pohl B, Wilda M, *et al*: Expression of the highly conserved RNA binding protein KOC in embryogenesis. Mech Dev 88: 95-99, 1999.
5. Yaniv K and Yisraeli JK: The involvement of a conserved family of RNA binding proteins in embryonic development and carcinogenesis. Gene 287: 49-54, 2002.
6. Gu L, Shigemasa K and Ohama K: Increased expression of IGF II mRNA-binding protein 1 mRNA is associated with an advanced clinical stage and poor prognosis in patients with ovarian cancer. Int J Oncol 24: 671-678, 2004.
7. Hammer NA, Hansen T, Byskov AG, *et al*: Expression of IGF-II mRNA-binding proteins (IMPs) in gonads and testicular cancer. Reproduction 130: 203-212, 2005.
8. Hoffmann NE, Sheinin Y, Lohse CM, *et al*: External validation of IMP3 expression as an independent prognostic marker for metastatic progression and death for patients with clear cell renal cell carcinoma. Cancer 112: 1471-1479, 2008.
9. Jiang Z, Chu PG, Woda BA, *et al*: Analysis of RNA-binding protein IMP3 to predict metastasis and prognosis of renal-cell carcinoma: a retrospective study. Lancet Oncol 7: 556-564, 2006.
10. Li D, Yan D, Tang H, *et al*: IMP3 is a novel prognostic marker that correlates with colon cancer progression and pathogenesis. Ann Surg Oncol 16: 3499-3506, 2009.
11. Okada K, Fujiwara Y, Nakamura Y, *et al*: Oncofetal protein, IMP3, a potential marker for prediction of postoperative peritoneal dissemination in gastric adenocarcinoma. J Surg Oncol 105: 780-785, 2012.
12. Simon R, Bourne PA, Yang Q, *et al*: Extrapulmonary small cell carcinomas express K homology domain containing protein overexpressed in cancer, but carcinoid tumors do not. Hum Pathol 38: 1178-1183, 2007.
13. Xu H, Bourne PA, Spaulding BO and Wang HL: High-grade neuroendocrine carcinomas of the lung express K homology domain containing protein overexpressed in cancer but carcinoid tumors do not. Hum Pathol 38: 555-563, 2007.
14. Yantiss RK, Woda BA, Fanger GR, *et al*: KOC (K homology domain containing protein overexpressed in cancer): a novel molecular marker that distinguishes between benign and malignant lesions of the pancreas. Am J Surg Pathol 29: 188-195, 2005.
15. Zheng W, Yi X, Fadare O, *et al*: The oncofetal protein IMP3: a novel biomarker for endometrial serous carcinoma. Am J Surg Pathol 32: 304-315, 2008.
16. Doyle GA, Betz NA, Leeds PF, *et al*: The c-myc coding region determinant-binding protein: a member of a family of KH domain RNA-binding proteins. Nucleic Acids Res 26: 5036-5044, 1998.
17. Gress TM, Müller-Pillasch F, Geng M, *et al*: A pancreatic cancer-specific expression profile. Oncogene 13: 1819-1830, 1996.
18. Liao B, Hu Y, Herrick DJ and Brewer G: The RNA-binding protein IMP3 is a translational activator of insulin-like growth factor II leader-3 mRNA during proliferation of human K562 leukemia cells. J Biol Chem 280: 18517-18524, 2005.
19. Runge S, Nielsen FC, Nielsen J, *et al*: H19 RNA binds four molecules of insulin-like growth factor II mRNA-binding protein. J Biol Chem 275: 29562-29569, 2000.
20. Mueller F, Bommer M, Lacher U, *et al*: KOC is a novel molecular indicator of malignancy. Br J Cancer 88: 699-701, 2003.
21. Sobin LH, Gospodarowicz MK and Wittekind C (eds). Oesophagus including oesophagogastric junction. In: International Union Against Cancer (UICC) TNM classification of Malignant Tumors. 7th edition. Wiley-Blackwell, New York, NY, pp66-72, 2009.
22. Hansen TV, Hammer NA, Nielsen J, *et al*: Dwarfism and impaired gut development in insulin-like growth factor II mRNA-binding protein 1-deficient mice. Mol Cell Biol 24: 4448-4464, 2004.
23. Chao W and D'Amore PA: IGF2: epigenetic regulation and role in development and disease. Cytokine Growth Factor Rev 19: 111-120, 2008.
24. Foulstone E, Prince S, Zaccheo O, *et al*: Insulin-like growth factor ligands, receptors, and binding proteins in cancer. J Pathol 205: 145-153, 2005.
25. Vikesaa J, Hansen TV, Jønson L, *et al*: RNA-binding IMPs promote cell adhesion and invadopodia formation. EMBO J 25: 1456-1468, 2006.
26. Jeng YM, Wang TH, Lu SH, Yuan RH and Hsu HC: Prognostic significance of insulin-like growth factor II mRNA-binding protein 3 expression in gastric adenocarcinoma. Br J Surg 96: 66-73, 2009.
27. Pryor JG, Bourne PA, Yang Q, *et al*: IMP3 is a novel progression marker in malignant melanoma. Mod Pathol 21: 431-437, 2008.
28. Yoshino K, Motoyama S, Koyota S, *et al*: Identification of insulin-like growth factor 2 mRNA-binding protein 3 as a radioresistance factor in squamous esophageal cancer cells. Dis Esophagus: Sep 18, 2012 (Epub ahead of print).
29. Nischalke HD, Schmitz V, Luda C, *et al*: Detection of IGF2BP3, HOXB7, and NEK2 mRNA expression in brush cytology specimens as a new diagnostic tool in patients with biliary strictures. PLoS One 7: e42141, 2012.
30. Kono K, Iinuma H, Akutsu Y, *et al*: Multicenter, phase II clinical trial of cancer vaccination for advanced esophageal cancer with three peptides derived from novel cancer-testis antigens. J Transl Med 10: 141, 2012.

# Clinicopathological Significance of Leucine-Rich α2-Glycoprotein-1 in Sera of Patients With Pancreatic Cancer

AQ1 *Kenta Furukawa, MD,* Koichi Kawamoto, MD, PhD,* Hidetoshi Eguchi, MD, PhD,* Masahiro Tanemura, MD, PhD,† Tsukasa Tanida, MD,* Yoshito Tomimaru, MD, PhD,* Hirofumi Akita, MD, PhD,* Naoki Hama, MD, PhD,* Hiroshi Wada, MD, PhD,* Shogo Kobayashi, MD, PhD,* Yuji Nonaka, MS,‡ Shinji Takamatsu, PhD,‡ Shinichiro Shinzaki, MD, PhD,‡ Takashi Kumada, MD, PhD,§ Shinji Satomura, PhD,‖ Toshifumi Ito, MD, PhD,¶ Satoshi Serada, PhD,# Tetsuji Naka, MD, PhD,# Masaki Mori, MD, PhD,* Yuichiro Doki, MD, PhD,* Eiji Miyoshi, MD, PhD,‡ and Hiroaki Nagano, MD, PhD**

**Objectives:** Leucine-rich α2-glycoprotein-1 (LRG-1) is an inflammatory protein. Serum LRG-1 levels can reportedly be used as a cancer biomarker for several types of carcinoma. In the present study, we investigated the clinical usefulness of serum LRG-1 levels as a biomarker of pancreatic cancer.

**Methods:** A total of 124 patients with pancreatic cancer, 35 patients with chronic pancreatitis (CP), and 144 healthy volunteers were enrolled in the study. Serum LRG-1 levels were assayed by enzyme-linked immunosorbent assay. Immunohistochemistry was used to examine LRG-1 expression in pancreatic cancer tissues.

**Results:** Serum LRG-1 levels were significantly increased in patients with pancreatic cancer compared with CP patients and healthy volunteers. The LRG-1 levels increased with progressive clinical stages of pancreatic cancer. Receiver operator curve analysis showed that a combination of carbohydrate antigen 19-9 and LRG-1 resulted in a higher area under the curve for the diagnosis of pancreatic cancer. Positive staining was observed in all cases of pancreatic cancer, but positive signal was scarcely detected in tissues from CP patients or normal surrounding tissue.

**Conclusions:** These results suggest that serum LRG-1 is a promising biomarker for pancreatic cancer.

**Key Words:** leucine-rich α2-glycoprotein-1, pancreatic cancer, biomarker

(*Pancreas* 2014;00: 00–00)

Pancreatic cancer is the fourth leading cause of cancer-related death in the United States.[1] Pancreatic ductal adenocarcinoma (PDAC) is the most common form of pancreatic cancer. In Japan, the mortality rate for PDAC has increased over the past decade, currently ranking fifth.[2] Pancreatic ductal adenocarcinoma has an extremely poor prognosis with a 5-year survival rate of less than 5%. Early detection of PDAC remains clinically challenging because of its asymptomatic nature, and surgery offers the only potential cure. However, the 5-year survival of PDAC patients after curative resection (surgery alone) is estimated to be 10% to 20%.[3] Curative surgery with adjuvant chemotherapy improves overall survival,[4] but the clinical outcome of pancreatic cancer has not been markedly improved. One strategy that could improve PDAC survival is to detect the cancer in its early clinical stages. Thus, there is an urgent need to develop biomarkers for the stratification of patients for current treatment modalities and the development of novel therapeutic strategies.

Molecules that are specifically overexpressed in tumors not only serve as useful diagnostic markers, but also as potential therapeutic targets.[5] The development of methods that are sensitive and specific enough to permit an early diagnosis of PDAC may facilitate the detection and subsequent treatment of this disease. However, an important factor adds another level of complexity to this already demanding task. A number of overlapping symptomatological features are known to link pancreatic adenocarcinoma to the inflammatory disease chronic pancreatitis (CP), often obscuring the distinction between these 2 pathological conditions.

Carcinoembryonic antigen, carbohydrate antigen 19-9 (CA19-9), and DUPAN-2 are the only serum biomarkers currently available for AQ3 PDAC detection and have shown some utility as diagnostic adjuncts and prognostic markers in Japan.[6] However, these markers are not widely used in routine clinical practice in Europe and America due to low sensitivity, specificity, or reproducibility and therefore cannot be routinely used to diagnose PDAC. Although CA19-9 is not a specific marker, identifying characteristic CA19-9 carrier proteins may allow higher specificity (molecular proteomics). Although the detection of CA19-9 carrier proteins is established, it will be very difficult to detect the early stage of pancreatic cancer.[7] To establish a next-generation biomarker for pancreatic cancer, combination assays of several cancer biomarkers or a novel type of cancer biomarker involved in CP will be required.

Leucine-rich α2-glycoprotein-1 (LRG-1) was first identified in 1977 as an inflammatory protein in human serum.[8] Recent studies have demonstrated that serum LRG-1 can be used as a biomarker in several kinds of cancer, including ovarian, lung, biliary tract, and hepatocellular carcinoma related to hepatitis B virus infection.[9–13] Increased serum LRG-1 levels in patients with pancreatic cancer were first reported using multidimensional liquid chromatography followed by 2-dimensional difference gel electrophoresis in plasma proteomics.[14] The authors used Western blot to confirm the increase in serum LRG-1 patients with pancreatic cancer compared with healthy volunteers (HVs), and they showed that patients with CP tended to express lower serum levels of LRG-1 than patients with PDAC. However, they did not find significant differences between patients with CP and patients with PDAC due, at least in part, to the limited number of patients in the study. The study did not investigate the relationships between the marker and the clinical stages of pancreatic cancer, and no immunological study of LRG-1 in pancreatic cancer was performed. As LRG-1 has also been reported to be part of an acute inflammatory

AQ2 From the *Department of Surgery, Osaka University Graduate School of Medicine, Osaka; †Department of Surgery and Institute for Clinical Research National Hospital Organization Kure Medical Center and Chugoku Cancer Center, Hiroshima; ‡Department of Molecular Biochemistry and Clinical Investigation, Osaka University Graduate School of Medicine, Osaka; §Department of Gastroenterology, Ogaki Municipal Hospital, Ogaki; ‖Wako Pure Chemical Industries, Ltd; ¶Department of Gastroenterology and Hepatology, Japan Community Health Care Organization Osaka Hospital; and #Laboratory for Immune Signal, National Institute of Biomedical Innovation, Osaka, Japan.

Received for publication November 25, 2013; accepted June 20, 2014.

Reprints: Hiroaki Nagano, MD, PhD, Department of Surgery, Osaka University, Graduate School of Medicine, Suita, Yamadaoka 2-2, Osaka 565-0871, Japan (e-mail: hnagano@gesurg.med.osaka-u.ac.jp).

The authors declare no conflict of interest.

response in ulcerative colitis and acute appendicitis, LRG-1 may be increased as a result of inflammation.[15–18]

In the present study, we determined serum LRG-1 levels in patients with CP and PDAC and assessed the clinicopathological significance of the increase in LRG-1 in terms of clinical parameters and immunohistochemistry.

## MATERIALS AND METHODS

### Patients and Sample Collection

Peripheral blood samples from patients with pancreatic disease and apparently HVs were obtained from Ogaki Municipal Hospital, Japan Community Health Care Organization Osaka Hospital, and Osaka University Hospital. Written informed consent was obtained from all patients and HVs. The study was performed in accordance with the guidelines issued by the local institutional review board of Osaka University. Sera from 124 patients with PDAC and 35 patients with CP were evaluated. All blood sampling was done at the time of diagnosis (pretreatment). A total of 144 serum samples from HVs were used as controls. Detailed information on clinical background was available for 71 PDAC patients, 20 CP patients, and 91 HVs. The collection, processing, and storage of all blood samples were standardized as follows: blood samples were collected in a vacutainer tube, allowed to clot at room temperature for 30 minutes, and then centrifuged at ~2500 × g for 10 minutes. The serum was removed and immediately divided into 100-μL and 1-mL aliquots and stored at −80°C until use.

Formalin-fixed, paraffin-embedded tissue blocks from patients with PDAC were obtained from surgical cases at Osaka University Hospital in 2011 and 2012. Eleven PDAC, 1 CP, and 3 noncystic lesions of intraductal papillary mucinous neoplasm (IPMN; control for normal pancreas) were randomly selected.

### Quantification of Serum LRG-1

Serum LRG-1 levels were determined using the human LRG assay kit (IBL, Fujioka, Japan) according to the manufacturer's protocol. Briefly, each serum sample was diluted (1:100) with buffer from the kit and the assays performed in triplicate. The LRG-1 levels were determined from a standard curve created using control samples. If the concentration of serum LRG-1 was less than 1.56 ng/mL or greater than 100 ng/mL, the dilution rate was changed.

Serum CA19-9 levels were measured in the hospital laboratory at the time of diagnosis.

### Statistical Analysis

All statistical analyses were performed using JMP (version 9.0; SAS Institute Inc, Japan). Continuous data between clinical groups were compared by the Mann-Whitney *U* test for nonparametric data and the Student *t* test for normally distributed data. The Pearson product–moment correlation coefficient was used to examine associations between 2 continuous variables. Associations between categorical variables were examined using Fisher exact test. Normal cutoffs were defined for LRG-1 as the optimum point at which sensitivity and specificity was maximized. Receiver operating characteristic (ROC) curves were generated, and the areas under the curve (AUCs) were defined.

### Immunohistochemical Staining

To analyze LRG-1 expression by immunohistochemistry, formalin-fixed, paraffin-embedded tissue blocks from patients with pancreatic cancer were deparaffinized in xylene and rinsed in a series of 100%, 95%, 90%, 80%, 70%, and 60% ethanol solutions. The antigen was recovered by incubating the slides in 10 mmol/L citrate buffer (pH 6.0) for 40 minutes in boiling water. To quench endogenous peroxidase activity, the slides were incubated with 0.3% $H_2O_2$ in methanol for 30 minutes and then rinsed extensively in phosphate-buffered saline. The slides were incubated with blocking serum for 20 minutes followed by a 1:400 dilution of rabbit anti-LRG monoclonal antibody (Cat# 13224-1-AP; ProteinTech Group, Chicago, Ill) overnight at 4°C. Endogenous biotin activity was blocked using an avidin D–biotin blocking solution before in situ localization of the antigen using a biotin-avidin antigen detection method (R.T.U. Vectastain kit, Vector Laboratories, Burlingame, Calif). After extensive washing in phosphate-buffered saline, sections were incubated in a diaminobenzidine solution (Stable DAB, Invitrogen, Carlsbad, Calif) and counterstained with a hematoxylin solution. The slides were then dehydrated by washing in ethanol and cleared in xylene. Cover slips were placed on the slides, which were evaluated for LRG-1 staining. The intensity of LRG-1 staining was scored on a scale of 0 to 2 (0, no staining; 1, moderate staining; 2, strong staining).

## RESULTS

### Quantification of Serum LRG-1 Levels

Serum LRG-1 levels were significantly elevated in patients with PDAC (7.99 [5.07] μg/mL) compared with HVs (3.51 [1.42] μg/mL) and patients with CP (4.96 [2.11] μg/mL) ($P < 0.001$; Fig. 1, Table 1). F1 T1

When 71 patients with pancreatic cancer were investigated in terms of clinical stage, the mean (SD) LRG-1 concentrations significantly increased with the progression of clinical stage as follows: 3.33 (0.66) μg/mL in stage I, 7.07 (4.18) μg/mL in stage II, 8.74 (5.86) μg/mL in stage III, and 8.72 (4.35) μg/mL in stage IV (Fig. 2). Among them, significant difference of the LRG-1 concentrations was observed between stage I and the other stages, but the differences between stage II and III, III and IV, and II and IV were not significant. The mean (SD) LRG-1 concentration was F2

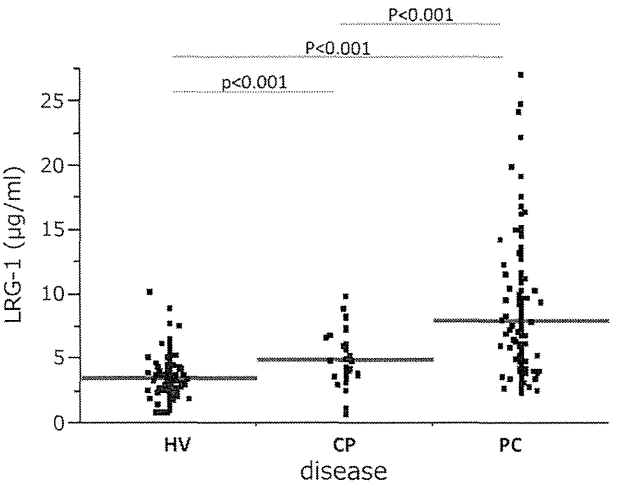


**FIGURE 1.** Detection of serum LRG-1 by enzyme-linked immunosorbent assay. Serum LRG-1 concentrations were determined for 124 patients with PDAC, 35 patients with CP, and 144 HVs. The mean (SD) LRG-1 concentration for PDAC patient sera was 7.99 (5.07) μg/mL compared with 3.51 (1.42) μg/mL for HV sera ($P < 0.001$) and 4.96 (2.11) μg/mL for CP patients ($P < 0.001$).

**TABLE 1.** Clinicopathological Characteristics of Patients With PDAC, HVs, and Patients With CP

| | PDAC (n = 124) | HV (n = 144) | CP (n = 35) | PDAC vs HV | PDAC vs CP |
|---|---|---|---|---|---|
| Age, y* | 66.4 (7.83) | 44.9 (12.5) | 66.7 (10.6) | $P < 0.01$ | NS |
| Sex, % male | 70.4 | 59.3 | 60.0 | NS | NS |
| LRG-1, μg/mL* | 7.99 (5.07) | 3.51 (1.42) | 4.96 (2.11) | $P < 0.01$ | $P < 0.01$ |
| CA19-9, U/mL* | 213.7 (208.1) | 13.3 (9.61) | 7.88 (8.88) | $P < 0.01$ | $P < 0.01$ |
| Tumor location (head/body, tail) | 42/29 | | | | |
| Lymph node metastasis (positive/negative) | 31/40 | | | | |
| Clinical stage (1/2/3/4)† | 6/28/21/16 | | | | |

*Data are presented as mean (SD).

AQ5 †General Rules for the Study of Pancreatic Cancer, 6th edition (Japan Pancreas Society).

NS indicates not significant.

significantly higher in the lymph node metastasis–positive group than AQ6 the lymph node metastasis–negative group (9.23 [4.68] μg/mL and 6.51 [4.69] μg/mL, respectively; $P < 0.001$). These results clearly demonstrate that in patients with PDAC, LRG-1 can be associated with local progression or lymph node metastasis of the primary tumor, but not with distant progression, such as liver metastasis. In addition, serum LRG-1 levels positively correlated with CA19-9 ($R^2 = 0.088$, $P < 0.001$), but not with carcinoembryonic antigen ($R^2 = 0.017$, $P = 0.27$).

## ROC Curve Analysis and Diagnostic Performance

The ROC curve analysis was performed to determine the clinical usefulness of LRG-1 for diagnosing pancreatic cancer. F3 As shown in Figure 3A, CA19-9 was useful for differentiating patients with PDAC from HVs with AUC of 0.869. At a cutoff value of 37 U/mL for CA19-9, the optimal sensitivity and specificity were 71.9% and 96.4%, respectively. Similar analysis indicated that the AUC for LRG-1 was 0.850. At a cutoff value of 4.81 μg/mL for LRG-1, the optimal sensitivity and specificity were 67.7% and 88.2%, respectively. The combination of LRG-1 and CA19-9 was analyzed by fixing the cutoff value at that of CA19-9. The combination of LRG-1 and CA19-9 improved the differential diagnosis between patients with PDAC and HVs, with an increase in AUC of 0.881 and 75.6% sensitivity and 91.7% specificity.

The ability of LRG-1 to make a differential diagnosis between patients with PDAC and patients with CP was also examined. The ROC curve analysis showed that AUC for CA19-9 was 0.913 (Fig. 3B). At a cutoff value of 37 U/mL for CA19-9, the optimal sensitivity and specificity were 73.7% and 100.0%, respectively. Similar analysis for LRG-1 showed AUC of 0.686. At a cutoff value of 4.81 μg/mL for LRG-1, the optimal sensitivity and specificity were 67.7% and 54.3%, respectively. The combination of LRG-1 and CA19-9 enhanced the differentiating power between patients with PDAC and patients with CP, with an increase in AUC to 0.942 with 75.6% sensitivity and 100.0% specificity.

In CA19-9–negative cases, the AUC for LRG-1 was 0.785. At a cutoff value of 4.81 μg/mL for LRG-1, the sensitivity and specificity in differentiating patients with PDAC from HVs were 68.8% and 86.3%, respectively. In regards to differentiating patients with PDAC from patients with CP, the AUC was 0.65, and the sensitivity and specificity were 68.8% and 50.0%, respectively.

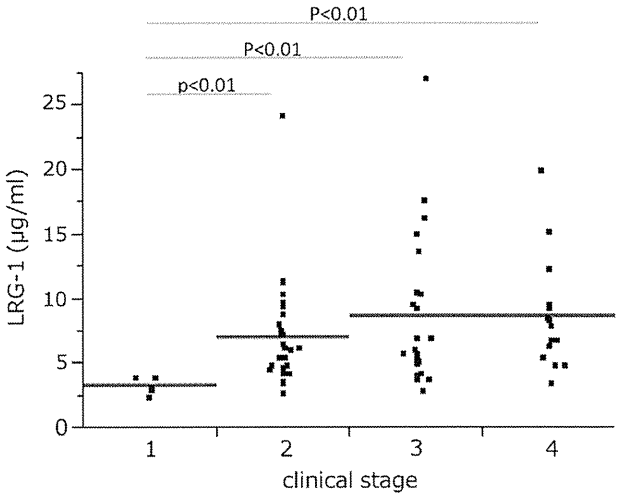


**FIGURE 2.** Detection of serum LRG-1 in pancreatic cancer patients by enzyme-linked immunosorbent assay. The mean (SD) LRG-1 concentration increased with the progression of clinical stage as follows: stage I, 3.33 (0.66) μg/mL; stage II, 7.07 (4.18) μg/mL; stage III, 8.74 (5.86) μg/mL; and stage IV, 8.72 (4.35) μg/mL. A significant difference was observed between stage I and the other stages, but the differences between stage II and III, III and IV, and II and IV were not significant.

## LRG-1 Immunohistochemistry

Serum cancer biomarkers can be produced by both cancer cells and the tissues surrounding them. Because LRG-1 is produced in the liver and white blood cells, it is important to identify which cells produce LRG-1 in pancreatic cancer tissue. To address this issue, the pattern of LRG-1 protein expression was assessed by immunohistochemistry using morphological cancer lesions and noncancerous lesions from resection tissue. As shown in Figure 4, pancreatic cancer cells stained positively on the cell sur- F4 face with a plasma membrane staining pattern, but pancreatic duct cells from noncancer cases, including CP and IPMN, did not stain. However, in CP cases, inflammatory cells such as lymphocytes exhibited weak staining. Positive staining was observed in all cases of pancreatic cancer, but a positive signal was scarcely detected in tissue from CP patients or normal surrounding tissue. Serum LRG-1 levels did not correlate with the intensity of immunostaining ($P = 0.327$).

## DISCUSSION

We demonstrated that preoperative serum LRG-1 levels are elevated in patients with PDAC compared with HVs and patients with CP. The LRG-1 level is associated with disease progression and

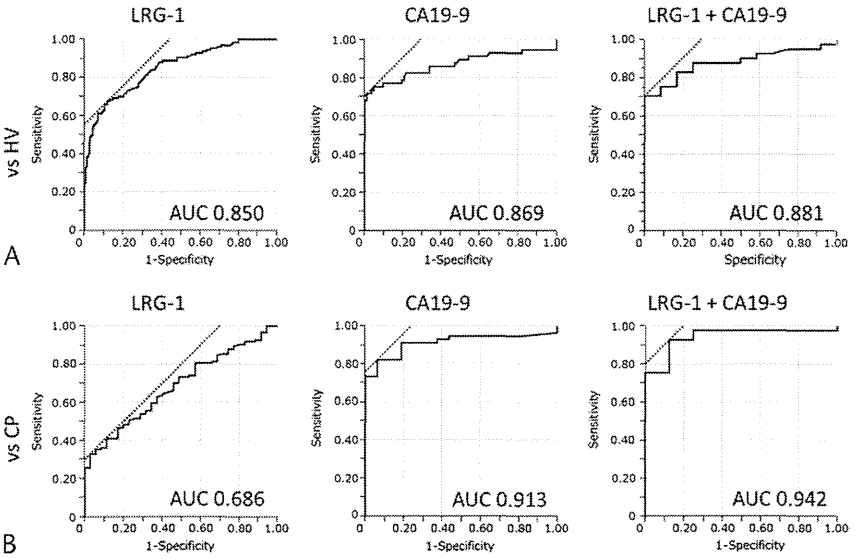


**FIGURE 3.** Receiver operating characteristic curve analysis for PDAC patients versus HVs (A) and PDAC patients versus CP patients (B). A, Power of LRG-1, CA19-9, and the combination of LRG-1 and CA19-9 in differentiating PDAC patients from HVs. The AUC was 0.850 for LRG-1 alone, 0.869 for CA19-9 alone, and 0.881 for LRG-1 and CA19-9 together. B, Power of LRG-1, CA19-9, and the combination of LRG-1 and CA19-9 in differentiating PDAC patients from CP patients. The AUC was 0.686 for LRG-1 alone, 0.913 for CA19-9 alone, and 0.942 for LRG-1 and CA19-9 together.

lymph node metastasis. Although previous studies have suggested that LRG-1 is induced by both tumor cells and acute/chronic inflammation, serum LRG-1 levels were not as high in the CP patients in our study as previously reported, dues in part to the mild/moderate levels of CP we investigated. Thus, the diagnosis of CP with mild inflammation may be difficult. In contrast, immunohistochemical staining clearly revealed that pancreatic cancer cells, but not noncancer lesions from CP and IPMN cases, were positive for LRG-1. This result suggests that high levels of LRG-1 in pancreatic cancer may be derived from cancer cells or a change in the microenvironment, such as local inflammation associated with cancer progression. However, serum LRG-1 levels did not correlate with staining intensity in tissues, suggesting that serum LRG-1 levels may be dependent on the cleavage of LRG-1 on the cell surface. Andersen et al[9] reported an association between LRG-1 and ovarian cancer. The mean serum LRG-1 concentration was higher in ovarian cancer patients than in healthy women, and highest among stage III/IV patients. Ovarian cancer cells secrete LRG-1, which may contribute directly to the elevated levels of LRG-1 observed in the serum of ovarian cancer patients. Interestingly, the time course is quite different for plasma LRG-1 and CA125. Suboptimal debulking surgery results in a substantial decrease in CA125, whereas LRG-1 levels remain elevated. Thus serum LRG-1 levels seem to be more directly related to tumor burden than CA125.

Initially, LRG-1 was classified as a marker of acute phase inflammatory responses. Serada et al[15] showed that serum LRG-1 concentrations correlate better with disease activity in ulcerative colitis than C-reactive protein. Kawakami et al[19] reported that LRG-1 levels increase after radiofrequency ablation for hepatocellular carcinoma, suggesting a possible role in the acute stress reaction. We confirmed an association between LRG-1 and C-reactive protein in patients with pancreatic cancer ($R^2 = 0.774$, $P < 0.001$). These dual functions of LRG-1 as a tumor marker and acute phase protein prompted us to use it as a marker of tumor recurrence after an acute phase.

We conducted this study to confirm that LRG-1 can be used as a diagnostic marker for PDAC. We found that LRG-1 can distinguish between patients with PDAC and HVs or patients with CP, but we were not able to demonstrate its effectiveness as an early diagnostic marker. However, we confirmed that serum LRG-1 levels are associated with disease progression and lymph node metastasis, and that pancreatic cancer cells express LRG-1 on the cell surface. An analysis of LRG-1 glycosylation may be a promising approach to distinguish cancer-associated LRG-1 from inflammation-associated LRG-1. In the future, if glycan changes in LRG-1 can be used to identify the pancreatic cancer-specific LRG-1, which is different from the LRG-1 protein made by normal cells such as hepatocytes, it may be a more specific biomarker in PDAC.

Leucine-rich α2-glycoprotein-1 was purified more than 30 years ago. The protein contains 8 typical 24-residue leucine-rich repeats with the consensus sequence.[20] However, the physiological function of LRG-1 is still largely unknown. Shirai et al[21] showed that autologous cytochrome *c* (cyt *c*) is an endogenous ligand of LRG-1 and functions in the detoxification of neurotoxins from snake venom. The expression of LRG-1 is up-regulated during neutrophilic granulocyte differentiation in response to G-CSF, suggesting that LRG-1 is involved in granulopoiesis. Leucine-rich α2-glycoprotein-1 functions as 1 of the pattern recognition receptors of polymorphonuclear neutrophils and modulates neutrophil function through innate immunity. Serum LRG-1 concentrations correlate well with disease activity in ulcerative colitis. Recent reports have also demonstrated the diagnostic value of LRG-1 in the urine of children with acute appendicitis. These results support the role of LRG-1 in inflammatory responses. Leucine-rich α2-glycoprotein-1 and Apaf-1 have some amino acid sequence homology, and LRG-1 binding to cyt *c* is similar to that of Apaf-1.[22] However, in contrast to Apaf-1, LRG-1 may clear potentially dangerous cyt *c*. This report suggests a role of LRG-1 in preventing lymphocyte death. When bound to extracellular cyt *c* released from apoptotic cells, serum LRG-1 acts as a survival factor for lymphocytes, and possibly other cells. Moreover, aberrant neovascularization contributes to diseases, such as cancer, and is the consequence of inappropriate angiogenic signaling. The epithelial growth factor receptor and vascular endothelial growth factor are related to angiogenesis, and targeted agents that are capable of

 

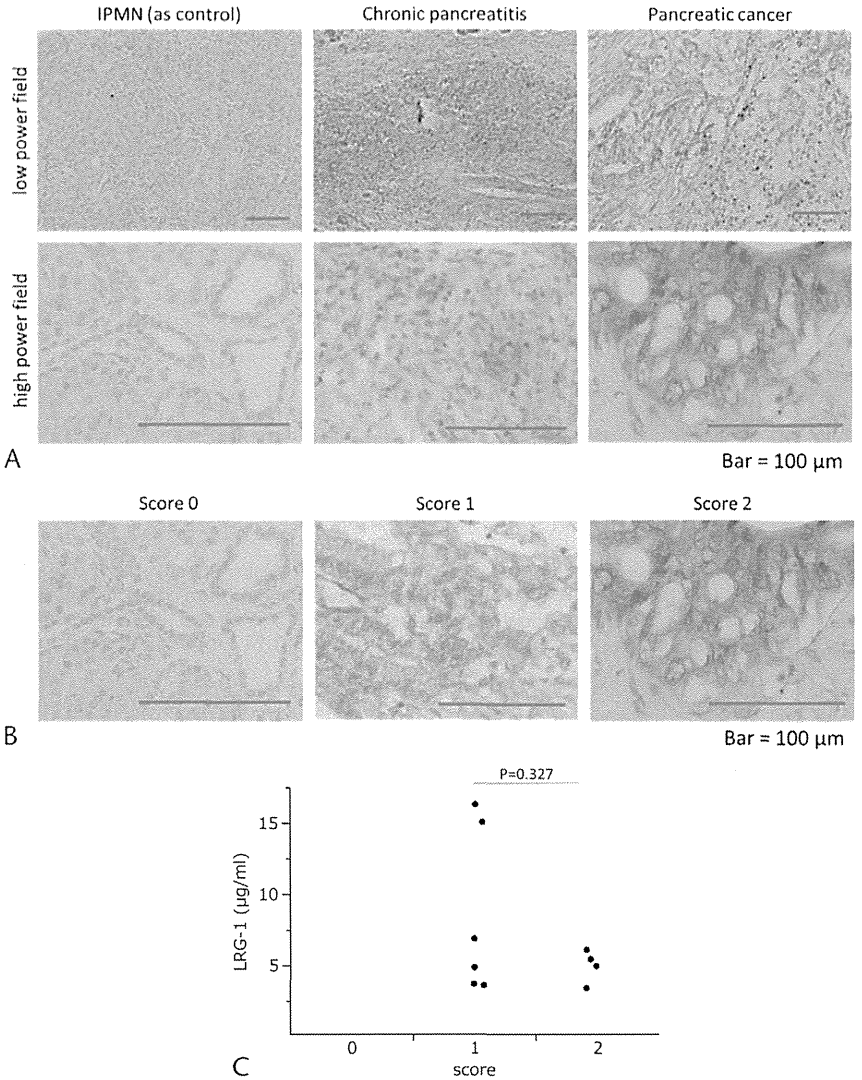


**FIGURE 4.** Immunohistochemistry of LRG-1 to assess the expression. A, In IPMN cases, the pancreatic duct cells were not stained. In the CP case, the pancreatic duct cells were not stained, but inflammatory cells, such as lymphocytes, stained lightly. In all PDAC cases, the pancreatic cancer cells were stained. Scale bar = 100 μm. B, The intensity of LRG-1 was scored on a scale from 0 to 2 (0, no or faint staining; 1, moderate staining; and 2, strong staining). Scale bar = 100 μm. C, No correlation was found between serum LRG-1 levels and staining intensity ($P = 0.327$).

inhibiting signal transduction through epithelial growth factor receptor and vascular endothelial growth factor have already been developed and are used clinically.[23] More recently, LRG-1 was reported to promote angiogenesis by modulating endothelial TGF-β signaling.[24] These results imply that LRG-1 may be a therapeutic target for controlling pathogenic angiogenesis in cancer.

In conclusion, the present study clearly shows that LRG-1 has promise as a novel tumor biomarker for PDAC.

## REFERENCES

1. Jemal A, Siegel R, Xu J, et al. Cancer Statistics, 2010. *CA Cancer J Clin.* 2011;61:133–134.
2. Ministry of Health, Labour and Welfare (2010). The Dynamic Statistics of the Population in 2010. Available at: http://www.mhlw.go.jp/toukei/saikin/hw/jinkou/kakutei11/dl/11_h7.pdf. Accessed December 12, 2012.
3. Wagner M, Redaelli C, Lietz M, et al. Curative resection is the single most important factor determining outcome in patients with pancreatic adenocarcinoma. *Br J Surg.* 2004;91:586–594.
4. Neoptolemos JP, Stocken DD, Bassi C, et al. Adjuvant chemotherapy with fluorouracil plus folinic acid vs gemcitabine following pancreatic cancer resection: a randomized controlled trial. *JAMA.* 2010;304:1073–1081.
5. Jamieson NB, Carter CR, McKay CJ, et al. Tissue biomarkers for prognosis in pancreatic ductal adenocarcinoma: a systematic review and meta-analysis. *Clin Cancer Res.* 2011;17:3316–3331.
6. Humphris JL, Chang DK, Johns AL, et al. The prognostic and predictive value of serum CA19-9 in pancreatic cancer. *Ann Oncol.* 2012;23:1713–1722.
7. Yachida S, Jones S, Bozic I. Distant metastasis occurs late during the genetic evolution of pancreatic cancer. *Nature.* 2010;467:1114–1117.
8. Haupt H, Baudner S. Isolation and characterization of an unknown, leucine-rich 3.1-S-alpha2-glycoprotein from human serum. *Hoppe Seylers Z Physiol Chem.* 1977;358:639–646.
9. Andersen JD, Boylan K, Jemmerson R, et al. Leucine-rich alpha-2-glycoprotein-1 is upregulated in sera and tumors of ovarian cancer patients. *J Ovarian Res.* 2010;3:21.

10. Okano T, Kondo T, Kakisaka T, et al. Plasma proteomics of lung cancer by a linkage of multi-dimensional liquid chromatography and two-dimensional difference gel electrophoresis. *Proteomics*. 2006;6:3938–3948.
11. Sandanayake NS, Sinclair J, Andreola F, et al. A combination of serum leucine-rich α-2-glycoprotein-1, CA19-9 and interleukin-6 differentiate biliary tract cancer from benign biliary strictures. *Br J Cancer*. 2011;105:1370–1378.
12. Sarvari J, Mojtahedi Z, Kuramitsu Y, et al. Differential expression of haptoglobin isoforms in chronic active hepatitis, cirrhosis and HCC related to HBV infection. *Oncol Lett*. 2011;2:871–877.
13. Ladd JJ, Busald T, Johnson MM, et al. Increased plasma levels of the APC-interacting protein MAPRE1, LRG1, and IGFBP2 preceding a diagnosis of colorectal cancer in women. *Cancer Prev Res (Phila)*. 2012;5:655–664.
14. Kakisaka T, Kondo T, Okano T, et al. Plasma proteomics of pancreatic cancer patients by multi-dimensional liquid chromatography and two-dimensional difference gel electrophoresis (2D-DIGE): up-regulation of leucine-rich alpha-2-glycoprotein in pancreatic cancer. *J Chromatogr B Analyt Technol Biomed Life Sci*. 2007;852:257–267.
15. Serada S, Fujimoto M, Terabe F, et al. Serum leucine-rich alpha-2 glycoprotein is a disease activity biomarker in ulcerative colitis. *Inflamm Bowel Dis*. 2012;18:2169–2179.
16. Kharbanda AB, Raj AJ, Cosme Y, et al. Novel serum and urine markers for pediatric appendicitis. *Acad Emerg Med*. 2012;19:56–62.
17. Ai J, Druhan LJ, Hunter MG, et al. LRG-accelerated differentiation defines unique G-CSFR signaling pathways downstream of PU.1 and C/EBPepsilon that modulate neutrophil activation. *J Leukoc Biol*. 2008;83:1277–1285.
18. Kentsis A, Ahmad S, Kurek K, et al. Detection and diagnostic value of urine leucine-rich α-2-glycoprotein in children with suspected acute appendicitis. *Ann Emerg Med*. 2012;60:78–83.
19. Kawakami T, Hoshida Y, Kanai F, et al. Proteomic analysis of sera from hepatocellular carcinoma patients after radiofrequency ablation treatment. *Proteomics*. 2005;5:4287–4295.
20. Takahashi N, Takahashi Y, Putnam FW. Periodicity of leucine and tandem repetition of a 24-amino acid segment in the primary structure of leucine-rich alpha 2-glycoprotein of human serum. *Proc Natl Acad Sci*. 1985;82:1906–1910.
21. Shirai R, Gotou R, Hirano F, et al. Autologous extracellular cytochrome c is an endogenous ligand for leucine-rich α2-glycoprotein and β-type phospholipase A2 inhibitor. *J Biol Chem*. 2010;285:21607–21614.
22. Codina R, Vanasse A, Kelekar A, et al. Cytochrome c-induced lymphocyte death from the outside in: inhibition by serum leucine-rich alpha-2-glycoprotein-1. *Apoptosis*. 2010;15:139–152.
23. Kim ST, Park KH, Shin SW, et al. Dose KRAS mutation status affect on the effect of VEGF therapy in metastatic colon cancer patients? *Cancer Res Treat*. 2014;46:48–54.
24. Wang X, Abraham S, McKenzie JA, et al. LRG1 promotes angiogenesis by modulating endothelial TGF-b signaling. *Nature*. 2013;499:306–311.

 

Rheumatology Advance Access published August 28, 2014
RHEUMATOLOGY 262
Original article doi:10.1093/rheumatology/keu325

# Proteomic identification of heterogeneous nuclear ribonucleoprotein K as a novel cold-associated autoantigen in patients with secondary Raynaud's phenomenon

**Lingli Yang[1,2], Minoru Fujimoto[2], Hiroyuki Murota[1], Satoshi Serada[2], Manabu Fujimoto[3], Hiromi Honda[2], Kohji Yamada[2,4], Katsuya Suzuki[5], Ayumi Nishikawa[5], Yuji Hosono[6], Yoshihiro Yoneda[7], Kazuhiko Takehara[3], Yoshitaka Imura[6], Tsuneyo Mimori[6], Tsutomu Takeuchi[5], Ichiro Katayama[1] and Tetsuji Naka[2]**

## Abstract

**Objective.** The aim of this study was to identify cold-associated autoantibodies in patients with RP secondary to CTDs.

**Methods.** Indirect immunofluorescence staining was performed on non-permeabilized cold-stimulated normal human dermal microvascular endothelial cells (dHMVECs), using patients' sera. Cold-induced alterations in cell surface proteomes were analysed by isobaric tag for relative and absolute quantitation (iTRAQ) analysis. Serological proteome analysis (SERPA) was applied to screen cold-associated autoantigens. The prevalence of the candidate autoantibody was determined by ELISA in 290 patients with RP secondary to CTDs (SSc, SLE or MCTD), 10 patients with primary RP and 27 healthy controls.

**Results.** Enhanced cell surface immunoreactivity was detected in cold-stimulated dHMVECs when incubated with sera from patients with secondary RP. By iTRAQ analysis, many proteins, including heterogeneous nuclear ribonucleoprotein K (hnRNP-K), were found to be increased on the cell surface of dHMVECs after cold stimulation. By the SERPA approach, hnRNP-K was identified as a candidate autoantigen in patients with secondary RP. Cold-induced translocation of hnRNP-K to the cell surface was confirmed by immunoblotting and flow cytometry. By ELISA analysis, patients with secondary RP show a significantly higher prevalence of anti-hnRNP-K autoantibody (30.0%, 61/203) than patients without RP (9.2%, 8/87, $P = 0.0001$), patients with primary RP (0%, 0/10, $P = 0.0314$) or healthy controls (0%, 0/27, $P = 0.0001$).

**Conclusion.** By comprehensive proteomics, we identified hnRNP-K as a novel cold-associated autoantigen in patients with secondary RP. Anti-hnRNP-K autoantibody may potentially serve as a biomarker for RP secondary to various CTDs.

**Key words:** proteomics, Raynaud's phenomenon, autoantibody, heterogeneous nuclear RNP-K.

[1]Department of Dermatology, Osaka University Graduate School of Medicine, [2]Laboratory of Immune Signal, National Institute of Biomedical Innovation, [3]Department of Dermatology, Kanazawa University, Kanazawa, [4]Biomolecular Dynamics Group, Graduate School of Frontier Biosciences, Osaka University, Osaka, [5]Division of Rheumatology, Department of Internal Medicine, Keio University School of Medicine, Tokyo, [6]Department of Rheumatology and Clinical Immunology, Graduate School of Medicine, Kyoto University, Kyoto and [7]National Institute of Biomedical Innovation, Osaka, Japan.

Submitted 4 November 2013; revised version accepted 23 June 2014.

Correspondence to: Tetsuji Naka, Laboratory of Immune Signal, National Institute of Biomedical Innovation, 7-6-8, Saito-asagi, Ibaraki, Osaka 567-0085, Japan. E-mail: tnaka@nibio.go.jp

Lingli Yang, Minoru Fujimoto, Hiroyuki Murota and Satoshi Serada contributed equally to this study.







BASIC SCIENCE

## Introduction

Advances in proteomics technologies have enabled us to identify proteins extracted from various clinical samples. Recently an innovative multiplexed quantitative proteomic technology called isobaric tag for relative and absolute quantification (iTRAQ) has been successfully used to detect disease-related proteins from cultured cells and clinical samples [1]. This novel technology can not only identify proteins in samples, but also compare relative expression levels of detected proteins from between four to eight different samples [2]. In addition, when samples enriched with cell surface proteins are analysed, iTRAQ technology can characterize differences in cell surface proteomes between samples [3].

RP is an exaggerated vasoconstrictive response of the fingers and toes to external stress such as cold temperatures [4]. RP is characterized classically as the episodic colour change of blanching, cyanosis and rubor in response to external stress [5]. In most patients, this colour change is a benign, reversible condition and no underlying disease is detectable (i.e. primary RP) [4]. However, in some patients RP is the early manifestation of underlying disease (i.e. secondary RP), most frequently of CTDs, including SSc [4], SLE [6] and MCTD [7]. RP in CTD patients is more severe than primary RP and causes tissue damage, including digital ulcers and gangrene, presumably due to endothelial abnormalities [8]. Moreover, given the substantial morbidity in patients with CTDs, RP patients developing CTDs should be promptly identified and managed. Thus it is important to distinguish between primary and secondary RP, but the diagnostic methods have not been established.

Because autoantibody production is a common hallmark of CTDs, RP secondary to CTDs might have a similar autoimmune pathogenesis. We therefore hypothesized that cold stimulation, as an environmental cue, may contribute to the triggering of local autoimmune reactions in patients with CTD-related secondary RP. In this study, taking advantage of iTRAQ technology, we detected cold-induced alteration in cell surface proteomes of endothelial cells. We then obtained candidate autoantigens in RP by serological proteome analysis (SERPA) [9–11] combining two-dimensional electrophoresis and western blotting using patients' sera. Our analyses collectively suggest that in patients with secondary RP, heterogeneous nuclear ribonucleoprotein K (hnRNP-K) is a cold-associated autoantigen that translocates onto the cell surface by cold stimulation.

## Materials and methods

### Human serum samples

Between March 2003 and January 2012, Japanese patients referred to hospitals of Osaka University (Osaka, Japan), Kyoto University (Kyoto, Japan), Kanazawa University (Kanazawa, Japan) and Keio University (Tokyo, Japan) were newly evaluated for RP as well as for SSc according to ACR criteria [12], SLE according to ACR criteria [13, 14] or MCTD according to the criteria proposed by the Ministry of Health and Welfare in Japan [15]. RP was defined by repeated episodes of biphasic or triphasic colour change on cold exposure and non-RP was defined by no colour changes on cold exposure, as described previously [16]. The possible RP of unilateral or uniphasic colour change was not included in this study. After these exclusions, randomly selected patients, including 155 well-defined SSc with RP [SSc-RP(+)] patients, 54 SLE without RP [SLE-RP(−)] patients, 1 MCTD without RP [MCTD-RP(−)] patient and 10 MCTD with RP [MCTD-RP(+)] patients, were included in this study. SSc without RP [SSc-RP(−)] patients ($n = 32$) and SLE with well-defined RP [SLE-RP(+)] ($n = 38$) patients, the frequencies of which are substantially low, were intentionally recruited and included in the study. Sera and characteristics (demographic characteristics, autoantibody profile) of CTD patients were collected at the time of diagnosis. Ten patients with primary RP who had well-defined RP for >2 years and had normal findings on laboratory tests, negative findings on autoantibody assays and no objective clinical signs of CTD or other diseases were also included. These patient characteristics are summarized in Table 1. As controls, healthy individuals with no evidence of any physical disorder were included [$n = 27$; male:female ratio 3:24, average age 51.0 years (S.D. 13.2)]. All patients gave written informed consent prior to inclusion and this study was approved by the Medical Ethics Committees of the National Institute of Biomedical Innovation (Osaka, Japan), Osaka University Hospital, Kyoto University Hospital, Kanazawa University Hospital and Keio University Hospital.

### Cell culture and cold stimulation

Normal human dermal microvascular (MV) endothelial cells (dHMVECs, passages 4–6) were purchased from Takara Bio (Otsu, Japan). dHMVECs were cultured on type 1 collagen-coated plates (Iwaki Glass, Tokyo, Japan) in endothelial basal medium 2 supplemented with endothelial cell growth medium 2 MV SingleQuots (Clonetics, San Diego, CA, USA). Confluent dHMVECs cells were incubated in serum-containing medium at 10°C (cold stress) or 37°C (control) in a 5% $CO_2$ humidified incubator for the periods indicated. Cells were maintained at 10°C or 37°C during the washing/detachment procedure. Suspended cells were then harvested by centrifugation at room temperature. Before and after cold stimulation, cell viability was verified by trypan blue exclusion assay. In some experiments, cells were further fixed with 4% paraformaldehyde at room temperature.

### Indirect immunofluorescence staining

dHMVECs were seeded on six-well plates precoated with type 1 collagen ($5 \times 10^4$ cells/well) and grown to confluence. Cells were fixed with 4% paraformaldehyde. Non-permeabilized cells were then incubated with sera from patients and healthy controls (HCs; 1:500 dilution) for 1 h at room temperature, followed by incubation with FITC-conjugated rabbit anti-human IgG (1:1000 dilution;

TABLE 1 Patient characteristics ($n = 300$ with CTDs or primary RP)

| Variable | SSc ($n = 187$) | SLE ($n = 92$) | MCTD ($n = 11$) | Primary RP ($n = 10$) |
|---|---|---|---|---|
| Age, mean (S.D.), years | 55.3 (13.8) | 40.3 (14.9) | 59.5 (16.3) | 25.4 (3.1) |
| Gender (F:M), *n:n* | 156:31 | 86:6 | 11:0 | 9:1 |
| Smoking, % (*n/N*) | 44.2 (50/163) | 25.8 (16/46) | 0 (0/11) | 0 (0/10) |
| ANA positivity, % (n/N) | 91.4 (167/183) | 96.7 (89/92) | 100 (10/10) | 0 (0) |
| Anti-Scl-70, % (*n/N*) | 31.0 (58/187) | NA | NA | 0 (0/10) |
| Anti-centromere, % (*n/N*) | 33.7 (63/187) | NA | 9.1 (1/11) | 0 (0/10) |
| Anti-Sm, % (*n/N*) | NA | 34.5 (30/87) | 9.1 (1/11) | NA |
| Anti-dsDNA, % (*n/N*) | NA | 65.1 (54/83) | 0 (0/3) | NA |
| Anti-U1-RNP, % (*n/N*) | 7.5 (14/187) | 50.0 (43/86) | 100.0 (11/11) | 0 (0/10) |
| Anti-SSA/Ro, % (*n/N*) | 7.5 (14/187) | 57.8 (52/87) | 45.5 (5/11) | NA |

Scl-70: topoisomerase I; Sm: Smith; U1-RNP: U1 ribonucleoprotein; *N*: the number of available patients (varies according to the number of available observations); NA: not available.

Dako Immunoglobulins, Copenhagen, Denmark). Cells counterstained with Hoechst 33342 (Invitrogen, Carlsbad, CA, USA) were visualized using a Biozero microscope (Keyence, Itasca, IL, USA).

### Capture of cell surface proteins

After cold stimulation (10°C) for the indicated periods (0 min, 30 min, 1 h, 3 h), dHMVECs were washed with pre-warmed (37°C) or precooled (10°C) PBS three times and cell surface proteins were then labelled by biotinylation and pulled down by avidin–agarose resin as described previously [3]. The isolated cell surface proteins were kept at −20°C until use.

### iTRAQ analysis

Cell surface proteins described above were digested by trypsin and separately labelled with the iTRAQ reagent (Applied Biosystems, Foster City, CA, USA) as described previously [3]. Briefly, iTRAQ reagents 114–117 were used to label cells without cold stimulation (baseline), cells with cold stimulation at 10°C for 30 min, cells with cold stimulation at 10°C for 1 h and cells with cold stimulation at 10°C for 3 h, respectively. Samples were then pooled and fractionated by strong cation exchange chromatography [3]. Nano liquid chromatography–tandem mass spectrometry (LC-MS/MS) analyses were performed on an LTQ-Orbitrap XL (Thermo Fisher Scientific, Waltham, MA, USA) as described previously [3]. Protein identification and quantification for iTRAQ analysis were carried out using Proteome Discoverer software (version 1.1; Thermo Fisher Scientific) against the Swiss Prot protein database [SwissProt 2010_10 (521 016 sequences)] as described previously [3] with modifications as follows: carbamidomethylation and iTRAQ4plex (Lys, N-terminal) were specified as static modifications, whereas CAMthiopropanoyl (Lys, N-terminal), iTRAQ4plex (Tyr) and oxidation (Met) were specified as variable modifications in the database search. The mass spectrometry raw data and the data of peptide identifications were uploaded to PeptideAtlas (http://www.peptideatlas.org/PASS/PASS00387). Information about the subcellular localization of detected proteins was obtained by using UniprotKB (http://www.uniprot.org/).

### Serological proteome analysis

Proteins were extracted from cultured dHMVECs using the Complete Mammalian Proteome Extraction Kit (Calbiochem, La Jolla, CA, USA) and stored at −80°C until use. Two-dimensional electrophoresis and immune blotting analysis using patient or HC sera were performed as previously described [10, 11]. Protein spots in a silver-stained gel, corresponding to positive spots on western blot membranes, were excised from the gel and digested in gel as described previously [17].

### Preparation of recombinant human hnRNP-K

Full-length hnRNP-K cDNA was amplified from total cDNA of dHMVEC using KOD-plus (Toyobo, Osaka, Japan) with the following primers: 5′-TGGAAACTGAACAGCCAGAAG AA-3′ (forward) and 5′-GCATTAGAATCCTTCAACATCTG C-3′ (reverse). Full-length hnRNP-K cDNA was subcloned into a pET28 vector (Novagen, Madison, WI, USA), resulting in expression of hnRNP-K with a 6 × His tag. The DNA sequence was confirmed using the ABI Prism 3130XL Genetic Analyzer (Applied Biosystems). Recombinant protein was produced in *Escherichia coli* as described previously [10, 11].

### ELISA

The ELISA assay was performed using MaxiSorp plates (Nunc A/S, Roskilde, Denmark) coated with 1 μg/well of recombinant human full-length hnRNP-K protein. After dilution (1:500) with *E. coli* cell lysates to block the non-specific reactivity of sera with bacterial proteins, sera were incubated with plate-bound hnRNP-K for 1 h, followed by detection of antigen–antibody complexes by horseradish peroxidase (HRP)-conjugated rabbit anti-human IgG (Dako, Carpinteria, CA, USA) as described previously [10, 11]. Optical density (OD) was read at 450 nm on a Model 680 Microplate Reader (Bio-Rad Laboratories, Hercules, CA, USA). The antibody titre was expressed using arbitrary binding units calculated

according to the following formula: binding units of sample = $[OD_{sample}/(\text{mean } OD_{HC\ sera} + 3\ S.D._{HC\ sera})] \times 100$. Based on this formula, 100 binding units was used as the cut-off point.

### Western blot analysis

Extracted proteins were subjected to western blot analysis as previously described [18] with the following antibodies: serum at 1:200 dilution; anti-hnRNP-K (1:500 dilution; Cell Signaling Technology, Danvers, MA, USA); anti-VE-cadherin (1:500 dilution; BD Transduction Laboratories, San Jose, CA, USA); anti-glyceraldehyde-3-phosphate dehydrogenase (GAPDH; 1:1000 dilution; Santa Cruz Biotechnology, Dallas, TX, USA), followed by rabbit anti-human IgG, donkey anti-rabbit or sheep anti-mouse HRP-conjugated secondary antibodies (1:5000 dilution; GE Healthcare, Piscataway, NJ, USA) and visualized with Western Lightning Plus ECL reagent (Perkin-Elmer, Boston, MA, USA).

### Fluorescence-activated cell sorting

After stimulation, cells fixed with 4% paraformaldehyde were incubated with rabbit anti-human hnRNP-K antibody at 1:100 dilution and labelled with FITC-conjugated goat anti-rabbit immunoglobulin (BD Biosciences, San Jose, CA, USA). Normal rabbit IgG was used as a control. Stained cells were analysed using a FACS Canto II cytometer (Becton-Dickinson, Mountain View, CA, USA) and the results were analysed using FlowJo software (TreeStar, Ashland, OR, USA).

### Statistical analysis

Continuous variables are expressed as mean (S.D.) and proportions were used for categorical variables. Means were compared with Student's *t*-test, highly skewed distributions were compared using the Mann–Whitney *U* test and proportions were compared using Fisher's exact test. Differences between groups were compared using the Kruskall–Wallis test followed by Steel's test. The data were entered and analysed using Excel statistical software (Microsoft, Redmond, WA, USA). Significance was defined as $P < 0.05$.

## Results

### Cold-induced autoimmune reactions on the cell surface

To determine whether cold can affect autoimmune reactions on the surface of vascular endothelial cells, non-permeabilized dHMVECs pretreated with or without cold stimulation were incubated with sera from patients with RP secondary to SSc or HCs. By indirect immunofluorescence staining using sera from patients, cell surface immunoreactivity was strongly induced in cold-stimulated dHMVECs (eight of nine patients with SSC-related RP; Fig. 1), but not in unstimulated cells. In contrast, no distinct immunostaining was observed in cold-stimulated or unstimulated cells when incubated with sera from HCs ($n = 3$; Fig. 1). These results indicate that pretreatment of dHMVECs with cold is critical in inducing the interaction between cell surface autoantigens and sera from patients.

FIG. 1 Indirect immunofluorescence staining

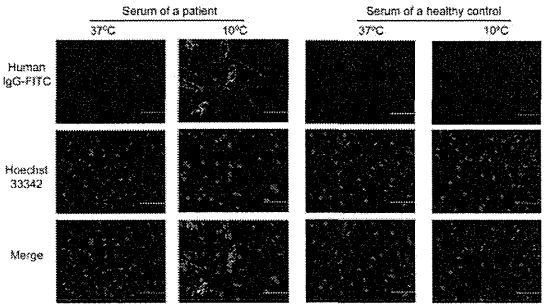


Non-permeabilized cultured dHMVECs with or without cold stimulation were incubated with sera (1:500 dilution) from patients with SSc-related secondary RP ($n = 9$) or healthy controls ($n = 3$) (×100 magnification). Representative images are shown here. FITC-conjugated rabbit anti-human IgG (green); Hoechst 33342 (blue); bar: 100 μm. dHMVECs: dermal human microvascular endothelial cells.

### Identification of cold-induced surface proteome alterations in dHMVECs by iTRAQ analysis

The results above suggest that proteins including autoantigens in dHMVECs might be exposed to the cell surface in response to cold stimulation. Therefore we next investigated cold-induced cell surface proteome alterations in dHMVECs. Cells were stimulated with cold (10°C for 0 min, 30 min, 1 h and 3 h) and cell surface proteins enriched by a biotinylation-based approach were quantitatively analysed by iTRAQ technology using nano LC-MS/MS analysis. As listed in supplementary Table S1, available at *Rheumatology* Online, 1581 proteins were identified. According to the annotation from UniprotKB, 451 proteins (28.5%) are located mainly in the plasma membrane, 503 proteins (31.8%) in the cytoplasm, 238 proteins (15.1%) in the nucleus and the remaining proteins (24.6%) in other subfractions such as the mitochondrion and the endoplasmic reticulum. The expression of ~50% of the proteins increased >2-fold after cold stimulation at 10°C for 3 h (see supplementary Table S1, available at *Rheumatology* Online). The top 30 highly increased proteins are listed in Table 2.

### Identification of autoantigens by SERPA in patients with secondary RP

We then used a SERPA approach to screen autoantigens associated with secondary RP. At first, proteins from dHMVEC lysates were separated on two-dimensional gels and were visualized by silver staining (Fig. 2A) or were transferred to membranes for immunoblotting. These membranes were incubated with sera from nine

TABLE 2 List of differentially expressed proteins on the cell surface of dHMVECs after cold stimulation

| Accession | Protein name | 0.5 h | 1 h | 3 h |
|---|---|---|---|---|
| Q96RS6 | NudC domain-containing protein 1 | 3.25 | 4.24 | 6.18 |
| P10301 | Ras-related protein R-Ras | 1.35 | 3.90 | 5.95 |
| Q92797 | Symplekin | 2.94 | 3.81 | 5.54 |
| Q643R3 | Lysophospholipid acyltranferase LPCAT4 | 3.06 | 3.00 | 5.45 |
| Q99808 | Equilibrative nucleoside transporter 1 | 2.62 | 3.69 | 5.21 |
| Q9Y6I9 | Testis-expressed sequence 264 protein | 2.66 | 4.11 | 5.12 |
| Q8TEQ6 | Gem-associated protein 5 | 4.71 | 6.03 | 5.08 |
| Q2TAL8 | Glutamine-rich protein 1 | 3.03 | 4.56 | 4.99 |
| Q08379 | Golgin subfamily A member 2 | 2.41 | 4.10 | 4.74 |
| P49916 | DNA ligase 3 | 2.52 | 2.94 | 4.74 |
| P35659 | Protein DEK | 2.04 | 3.65 | 4.67 |
| O60264 | SWI/SNF-related matrix-associated actin-dependent regulator of chromatin subfamily A member 5 | 1.87 | 4.38 | 4.52 |
| P60709 | Actin, cytoplasmic 1 | 3.03 | 3.67 | 4.28 |
| P55265 | Double-stranded RNA-specific adenosine deaminase | 2.22 | 3.86 | 4.27 |
| Q16643 | Drebrin | 2.60 | 3.75 | 4.24 |
| Q6DD88 | Atlastin-3 | 2.09 | 3.83 | 4.14 |
| P29966 | Myristoylated alanine-rich C-kinase substrate | 1.89 | 3.61 | 4.10 |
| Q9ULT8 | E3 ubiquitin-protein ligase HECTD1 | 1.74 | 3.63 | 4.08 |
| P61019 | Ras-related protein Rab-2A | 2.04 | 3.63 | 4.03 |
| P61978 | hnRNP-K | 2.12 | 3.75 | 4.03 |
| P01112 | GTPase HRas | 1.68 | 2.01 | 3.95 |
| Q07666 | KH domain-containing, RNA-binding, signal transduction-associated protein 1 | 1.74 | 3.54 | 3.92 |
| Q9NZ01 | Trans-2,3-enoyl-CoA reductase | 1.77 | 2.08 | 3.89 |
| Q9NQW6 | Actin-binding protein anillin | 3.78 | 5.01 | 3.86 |
| O00483 | NADH dehydrogenase [ubiquinone] 1 alpha subcomplex subunit 4 | 2.12 | 2.94 | 3.86 |
| Q9NP72 | Ras-related protein Rab-18 | 1.96 | 3.20 | 3.83 |
| O94901 | Protein unc-84 homolog A | 2.04 | 2.77 | 3.79 |
| P38646 | Stress-70 protein, mitochondrial | 1.83 | 3.39 | 3.76 |
| Q96S97 | Myeloid-associated differentiation marker | 2.49 | 3.10 | 3.75 |
| P49585 | Choline-phosphate cytidylyltransferase A | 2.68 | 3.62 | 3.74 |

Values are shown as relative expression levels (at 10°C for 0.5, 1 and 3 h) compared with baseline (at 37°C). dHMVECs: dermal human microvascular endothelial cells; hnRNP-K: heterogeneous nuclear ribonucleoprotein K.

patients with RP secondary to SSc (Fig. 2B) or three HCs (Fig. 2C). Six specific spots, which were recognized by sera from >75% of patients, but not by those from HCs, were selected (Fig. 2B). Proteins extracted from the corresponding spots on the silver-stained gel (Fig. 2A) were then subjected to LC-MS/MS analysis and candidate autoantigens were identified by a database search as detailed in Fig. 2D. Among identified candidates, hnRNP-K, a member of the nuclear proteins involved in nucleic acid metabolism [19], was also found in the list of increased proteins on the cell surface under cold stimulation (Table 2), suggesting that hnRNP-K might be a cold-related autoantigen in patients with secondary RP.

### Cell surface expression of hnRNP-K under cold stimulation was confirmed by western blot and FACS analysis

The hnRNP proteins are among the most abundant proteins in the nucleus [20]. Indeed, hnRNP-K in dHMVECs under physiological culture conditions was stained intensely in the nucleus by immunofluorescence analysis (see supplementary Fig. S1A and B, available at *Rheumatology* Online). Cold stimulation (10°C for 3 h) induced extranuclear localization of hnRNP-K (see supplementary Fig. S1C and D, available at *Rheumatology* Online), which was nonetheless overwhelmed by intensive staining of nuclear hnRNP-K. To investigate further the appearance of hnRNP-K on the cell surface after cold stimulation, we next performed western blot and FACS analysis. By western blot analysis using concentrated cell surface proteins, hnRNP-K clearly increased in dHMVECs after cold stimulation, but VE-cadherin did not (Fig. 3A). In contrast, the expression level of total hnRNP-K was found to be unchanged during cold stimulation, suggesting that hnRNP-K was not newly synthesized after cold stimulation (Fig. 3A). By FACS analysis, cold-induced expression of hnRNP-K on the cell surface was further confirmed (Fig. 3B). These results collectively suggest that hnRNP-K is a protein that translocates to the cell surface on cold stimulation.

FIG. 2 Identification of autoantigens by SERPA

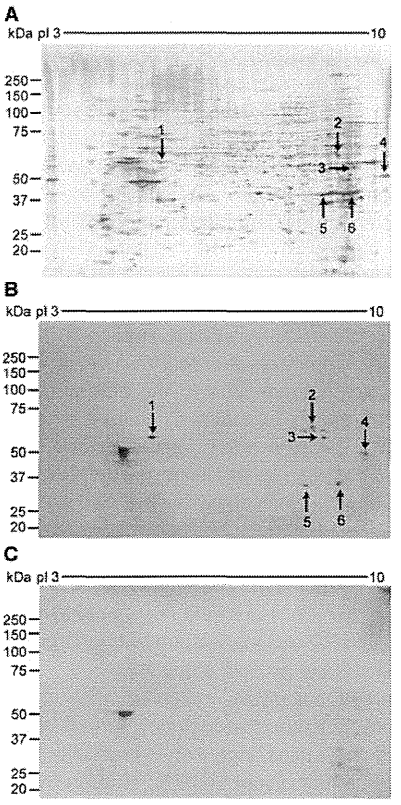


D

| no | Access | Identified protein | Mw(kDa) | PI | Coverage(%) |
|---|---|---|---|---|---|
| 1 | P48643 | T-complex protein 1 subunit epsilon | 59.63 | 5.66 | 30.13 |
| | P61978 | Heterogeneous nuclear ribonucleoprotein K | 50.94 | 5.54 | 19.44 |
| | P10809 | 60 kDa heat shock protein, mitochondrial | 61.92 | 5.87 | 16.40 |
| | Q13283 | Ras GTPase-activating protein-binding protein 1 | 52.13 | 5.52 | 18.03 |
| | Q92769 | Histone deacetylase 2 | 55.33 | 5.91 | 13.11 |
| | Q9H0R6 | Glutamyl-tRNA(Gln) amidotransferase subunit A homolog | 57.42 | 5.66 | 11.55 |
| | Q05682 | Caldesmon | 93.19 | 5.67 | 3.15 |
| | O15460 | Prolyl 4-hydroxylase subunit alpha-2 | 60.86 | 5.71 | 4.11 |
| | Q9UN86 | Ras GTPase-activating protein-binding protein 2 | 54.09 | 5.55 | 5.19 |
| 2 | P29401 | Transketolase | 67.83 | 7.66 | 8.19 |
| | P49748 | Very long-chain specific acyl-CoA dehydrogenase, mitochondrial | 70.35 | 8.75 | 4.27 |
| | Q92804 | TATA-binding protein-associated factor 2N | 61.79 | 8.02 | 7.77 |
| 3 | P14618 | Pyruvate kinase isozymes M1/M2 | 57.90 | 7.84 | 25.05 |
| | P50991 | T-complex protein 1 subunit delta | 57.89 | 7.83 | 11.13 |
| | Q14554 | Protein disulfide-isomerase A5 | 59.56 | 7.91 | 11.75 |
| | Q99832 | T-complex protein 1 subunit eta | 59.33 | 7.65 | 11.60 |
| | Q9H078 | Caseinolytic peptidase B protein homolog | 78.68 | 9.01 | 7.64 |
| | P06744 | Glucose-6-phosphate isomerase | 63.11 | 8.32 | 4.30 |
| 4 | P68104 | Elongation factor 1-alpha 1 | 50.11 | 9.01 | 16.45 |
| | P06733 | Alpha-enolase | 47.14 | 7.39 | 9.45 |
| | P55084 | Trifunctional enzyme subunit beta, mitochondrial | 51.26 | 9.41 | 6.12 |
| 5 | P00338 | L-lactate dehydrogenase A chain | 36.67 | 8.27 | 33.13 |
| | Q14192 | Four and a half LIM domains protein 2 | 32.17 | 7.55 | 34.41 |
| | P07355 | Annexin A2 | 38.58 | 7.75 | 20.06 |
| | P40926 | Malate dehydrogenase, mitochondrial | 35.48 | 8.68 | 18.05 |
| | P22626 | Heterogeneous nuclear ribonucleoproteins A2/B1 | 37.41 | 8.95 | 10.20 |
| | P53597 | Succinyl-CoA ligase [GDP-forming] subunit alpha, mitochondrial | 36.23 | 8.79 | 8.67 |
| | Q16270 | Insulin-like growth factor-binding protein 7 | 29.11 | 7.90 | 11.70 |
| 6 | P04406 | Glyceraldehyde-3-phosphate dehydrogenase | 36.03 | 8.46 | 11.94 |
| | P22626 | Heterogeneous nuclear ribonucleoproteins A2/B1 | 37.41 | 8.95 | 10.76 |
| | Q9UKM9 | RNA-binding protein Raly | 32.44 | 9.17 | 8.82 |
| | P23193 | Transcription elongation factor A protein 1 | 33.95 | 8.38 | 10.30 |
| | P07355 | Annexin A2 | 38.58 | 7.75 | 6.19 |

(**A**–**C**) Total protein extracts of dHMVECs were separated by two-dimensional PAGE followed by silver staining analysis (**A**) or by western blot analysis with diluted sera from SSc patients with RP (**B**) or from healthy controls (**C**). Arrows and numbers indicate protein spots that were recognized only by the patients' sera. Representative images are shown here. (**D**) List of proteins identified by LC-MS/MS analysis (Mw: molecular weight; pI: isoelectric point). dHMVECs: dermal human microvascular endothelial cells; LC-MS/MS: liquid chromatography–tandem mass spectrometry.

### Detection of anti-hnRNP-K antibody in sera from patients with secondary RP by western blot and ELISA analysis

To confirm that hnRNP-K is the autoantigen recognized by sera from patients with secondary RP, full-length recombinant human hnRNP-K protein was prepared and subjected to western blot analysis. As disease controls, SSc patients without RP were intentionally recruited to the study and their sera were investigated. Notably, intense reactivity against recombinant hnRNP-K protein was visualized in sera from SSc patients with RP, but not sera from SSc patients without RP or from HCs (Fig. 3C). This result implies that anti-hnRNP-K antibody is relevant to RP rather than to SSc itself.

We then developed an ELISA system using recombinant hnRNP-K protein to screen anti-hnRNP-K antibody in various CTD patients (SSc, SLE and MCTD) with or without RP and in patients with primary RP (Table 1). As shown in Fig. 3D (top), ELISA analysis revealed that significant elevations of anti-hnRNP-K antibody levels were observed in patients with SSc-, SLE- and MCTD-related RP, but not in patients without RP or those with primary RP compared with HCs (Fig. 3D, top). The prevalence of autoantibodies against hnRNP-K was 26.5% in SSc patients with RP, 42.1% in SLE patients with RP and 40.0% in MCTD patients with RP. In contrast, anti-hnRNP-K positivity was markedly low in CTD patients without RP and was 0% in primary RP patients and HCs (Fig. 3D, top). These results suggest that anti-hnRNP-K antibody is relevant to CTD-related secondary RP rather than to a single CTD.

Of all the CTDs (SSc, SLE and MCTD) in this study, a 30.0% prevalence of anti-hnRNP-K antibody was observed in patients with RP, much higher than that in patients without RP (9.20%, $P = 0.0001$), in patients with primary RP (0%, $P = 0.0314$) or in HCs (0%, $P = 0.0003$) (Fig. 3D, bottom). Anti-hnRNP-K-positive CTD patients had a significantly higher prevalence of RP (88.4%) than

FIG. 3 Cell surface expression of hnRNP-K after cold stimulation and the presence of anti-hnRNP-K autoantibody in sera from patients with secondary RP

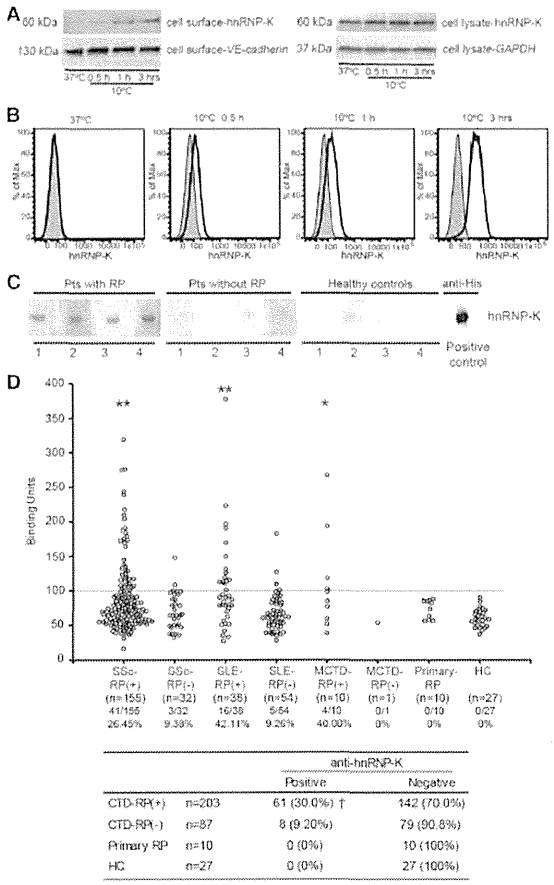


| | | anti-hnRNP-K | |
|---|---|---|---|
| | | Positive | Negative |
| CTD-RP(+) | n=203 | 61 (30.0%) † | 142 (70.0%) |
| CTD-RP(-) | n=87 | 8 (9.20%) | 79 (90.8%) |
| Primary RP | n=10 | 0 (0%) | 10 (100%) |
| HC | n=27 | 0 (0%) | 27 (100%) |

(**A**) Biotinylated surface proteins from dHMVECs incubated at 37°C or 10°C (indicated periods) were precipitated with streptavidin-conjugated agarose beads and analysed by western blot analysis using anti-hnRNP-K. Levels of VE-cadherin surface protein (left panel) and GAPDH expression in total cell lysates (right panel) are shown as controls. (**B**) Cell surface hnRNP-K expression in dHMVECs was analysed by flow cytometry. Shaded histogram indicates staining with control IgG. (**C**) His-tagged recombinant hnRNP-K protein was subjected to western blot analysis using diluted sera from SSc patients with RP, without RP and healthy controls or with anti-6 × His antibody. (**D**) (Top) Serum anti-hnRNP-K antibody levels in indicated CTD patients (with or without RP), primary RP patients and healthy controls were determined by ELISA using recombinant human hnRNP-K. The *y*-axis denotes binding units. The solid horizontal line indicates the positive cut-off limit as described in Materials and methods. Note that this cohort contains a relatively high number of SSc without RP patients and SLE with RP patients, because those patients were intentionally recruited to this study. $^{*}P < 0.05$, $^{**}P < 0.01$ *vs* HCs. (Bottom) Anti-hnRNP-K positivity in patients is summarized. CTD patients are combined here. Values are the number (%) of patients. †$P = 0.00001$ *vs* CTD-RP(−), $P = 0.0314$ *vs* primary RP, $P = 0.0001$ *vs* HCs by Fisher's exact test.
dHMVECs: dermal human microvascular endothelial cells; hnRNP-K: heterogeneous nuclear ribonucleoprotein K; GAPDH: glyceraldehyde-3-phosphate dehydrogenase.

anti-hnRNP-K-negative patients (64.3%, $P = 0.0001$; Table 3). Anti-hnRNP-K antibody showed no correlation with age, gender, smoking or antibodies to U1 ribonucleoprotein (U1-RNP), centromere or SSA/Ro in CTD patients (Table 3). In addition, anti-hnRNP-K showed no correlation with autoantibodies against topoisomerase I (Scl-70) in SSc patients or those against dsDNA or Sm in SLE patients (data not shown). Thus anti-hnRNP-K antibody might be a novel class of biomarker for a subgroup of patients with CTD-related secondary RP.

## Discussion

Environmental factors are implicated in the pathogenesis of autoimmune diseases. Previously translocation of intracellular autoantigens to the cell surface was described in ultraviolet radiation-stimulated keratinocytes [21–23]. In the present study, using comprehensive proteomics approaches, we identified hnRNP-K as a novel autoantigen that translocates to the cell surface of dHMVECs after cold stimulation. ELISA analysis revealed that anti-hnRNP-K antibody was significantly elevated in patients with RP secondary to CTDs, but not in patients with primary RP. Thus our data imply hnRNP-K is a putative secondary RP-associated autoantigen that is exposed on the cell surface by cold stimulation.

iTRAQ analysis indicated that cold stimulation in dHMVECs could induce cell surface expression of a variety of proteins, including intracellular proteins, without an overt effect on cell viability, as seen by trypan blue exclusion assay (data not shown). Previous lines of evidence indicate that cytoplasmic and nuclear proteins can reach the cell surface by Golgi-independent non-conventional transport pathways [24–26]. However, it is unknown how cold stimulation induces the translocation of hnRNP-K and other intracellular proteins. Further study is currently under way in our laboratory.

Among many up-regulated proteins identified by iTRAQ analysis, hnRNP-K was the only protein simultaneously identified by SERPA screening. However, our study does not exclude the possibility that there remain other cold-associated autoantigens among these proteins. In particular, since the SERPA approach has limitations in detecting native antigens, antibodies that recognize only native-form autoantigens might have been missed in our study. A screening strategy other than SERPA is necessary to clarify this issue.

hnRNP-K is a 464 amino acid nuclear protein with three K homology domains that mediate DNA and RNA binding [27]. Autoantibodies to hnRNP-K have previously been detected in sera from patients with aplastic anaemia and